T H E U N I V E R S I T Y O F M I C H I G A N

COLLEGE OF ENGINEERING
Department of Electrical Engineering
Space Physics Research Laboratory

Final Report

THE ACOUSTIC WIND MEASUREMENT

Prepared on behalf of the project by

D. L. Jones
G. M. Kakli
G. R. Carignan

ORA Project 07871

under contract with:

NATIONAL AERONAUTICS AND SPACE ADMINISTRATION
GEORGE C. MARSHALL SPACE FLIGHT CENTER
CONTRACT NO. NAS8-20357
HUNTSVILLE, ALABAMA

administered through:

OFFICE OF RESEARCH ADMINISTRATION ANN ARBOR

June 1969

ACKNOWLEDGMENTS

We wish to thank J. Nelson and W. Perry of the NASA George C. Marshall Space Flight Center for their assistance in the fabrication and operation of the microphone array, and Gary Poole of the Space Physics Research Laboratory, The University of Michigan, for programming the cross-correlation and the wind computations.

TABLE OF CONTENTS

	Page
LIST OF ILLUSTRATIONS	v
1. INTRODUCTION	1
2. DESCRIPTION OF THE EXPERIMENT	3
2.1. Instrumentation	3
2.2. Reduction of the Data	8
2.2.1. Microphone output cross-correlation	12
2.2.2. Wind computation	20
3. WIND PROFILES	25
4. FAR-FIELD ACOUSTIC WIND MEASUREMENT	44
5. SUMMARY	50
6. BIBLIOGRAPHY	52

LIST OF ILLUSTRATIONS

Table		Page
I.	Microphone Coordinates	4
II.	Rocket Launch Data	27

Figure

1.	Microphone array.	5
2.	Block diagram of acoustic wind measurement system.	6
3.	Hot-wire microphones and control panel.	7
4.	A typical microphone output.	10
5.	Geometry of the wind experiment showing time relationships for the j^{th} noise event.	11
6.	Variation of cross-correlation coefficient with time difference for a typical microphone pair.	17
7.	General flow of the cross-correlation program.	18
8.	Algorithm for finding t_o'.	19
9.	Flow diagram for wind computation.	24
10.	Wind profile, SA-9, 16 February 1965.	28
11.	Wind profile, Ranger 8, 17 February 1965.	29
12.	Wind profile, SA-8, 25 May 1965.	30
13.	Wind profile, SA-10, 30 July 1965.	31
14.	Wind profile, AS-201, 26 February 1966.	32
15.	Wind profile, AS-203, 5 July 1966.	33
16.	Wind profile, AS-202, 25 August 1966.	34

LIST OF ILLUSTRATIONS (Concluded)

Figure		Page
17.	Wind profile, Titan IIIC, 26 August 1966.	35
18.	Wind profile, Atlas Agena, 5 November 1967.	36
19.	Wind profile, AS-501, 9 November 1967.	37
20.	Wind profile, AS-204, 22 January 1968.	38
21.	Wind profile, AS-502, 4 April 1968.	39
22.	Wind profile, AS-205, 11 October 1968.	40
23.	Wind profile, Delta 63, 19 December 1968.	41
24.	Wind profile, AS-503, 21 December 1968.	42
25.	Wind profile, AS-504, 3 March 1969.	43
26.	Incoming acoustic wavefront.	45

1. INTRODUCTION

The present report summarizes the work accomplished under Contract NAS 8-20357 with the George C. Marshall Space Flight Center for the development of an acoustic wind measuring technique utilizing the exhaust noise of large booster rockets. The work is a continuation of earlier work, performed under Contract NAS8-11054, which investigated the feasibility of an acoustic wind measuring technique developed at the Space Physics Research Laboratory, The University of Michigan.

Under the initial contract the acoustic technique was successfully employed to determine wind profiles over Cape Kennedy from 0 to 85 km (Bushman, Kakli, and Carignan, 1965). The method, an extension of the rocket grenade experiment (Stroud, Nordberg, and Walsh, 1956; Nordberg and Smith, 1964), utilizes as its sound source the acoustic noise of large rocket engines instead of that of the grenade. In the rocket grenade experiment, discrete sound events occur at accurately known positions, and the times and the angles of arrival of these events at a ground-based microphone array are used to determine the atmospheric winds and the temperature in the layers between grenade detonations. When rocket exhaust noise is used as a sound source, because of its continuous nature, neither the time nor the location of the origin of the sound received at any given instant is known. If, however, the temperature profile is measured independently and the vehicle trajectory is known, then for any number of points (noise events), a correspondence can be established between the sound arrival times at the array and the exact loca-

tion of the sound source. The numerical evaluation of this relationship yields the average horizontal winds between adjacent noise events. Thus a wind profile is developed in a horizontally stratified model of the atmosphere, giving the average wind in each layer between selected noise events.

Since its inception in 1965, this technique has been used to compute wind profiles on 19 rocket firings. The data taken to date have demonstrated the meteorological usefulness of the method and agree favorably with profiles measured by other methods. The launches covered were not frequent enough to establish a seasonal trend, but the system is now operational and all launches at Cape Kennedy will be recorded as a matter of routine so that seasonal averages will be readily available.

2. DESCRIPTION OF THE EXPERIMENT

The basic experiment and theory have been well documented in previous reports (Milne, 1921; Groves, 1956; Bushman, Kakli, and Carignan, 1965; Otterman, 1958). Although the basic method of wind computation has not changed, the programs for calculating the winds have been modified to make the system more efficient and to require less computer time. The measurement equipment at Cape Kennedy has been improved to the point of being a permanent operational system. New weatherproof wiring has been installed from the blockhouse to the microphone array and all support electronics have been hardwired into the system (Figures 1, 2, and 3).

2.1. INSTRUMENTATION

A permanently established system for acoustic wind measurements consisting of a cross-shaped array of nine microphones has been set up on the southeast point of Cape Kennedy. A minimum of three microphones is required; the additional six microphones afford increased accuracy through use of statistical techniques and provide redundancy. The size of the microphone array, shown in Figure 1, is about 1200 meters along each axis. The size is chosen on the basis of optimizing two size-dependent error parameters, namely, (1) errors that decrease with increasing array-size introduced by finite resolution in measuring arrival times, and (2) errors that increase with increasing array-size introduced by the plane wave assumptions and practical considerations of suitable geography.

The microphones are hot-wire, single chamber Helmholtz resonators tuned

to about 4 Hz. These microphones, developed at The University of Texas at El Paso, have been used extensively in the rocket grenade experiment. Each microphone is contained in a concrete canister, recessed so that its top is level with the ground surface. The microphones are situated in heavily foliated areas to minimize local wind noise. The locations of the microphones have been surveyed to define accurately their geodetic position (see Table I). The microphones are connected by means of shielded weatherproof cables to a blockhouse containing support electronics and equipment for recording the microphone outputs (Figure 2). The outputs pass through variable attenuation to a magnetic tape recorder and are simultaneously recorded with range timing. The tape is then digitized and automatically reduced to wind profiles. The outputs are also monitored by an oscilloscope for quick look analysis and detection of any anomalies in the system.

TABLE I

MICROPHONE COORDINATES

Microphone Number	Longitude (West)	Latitude (North)	X (Meters)	Y (Meters)	Z (Meters)
1	80°32'03.933"	28°27'27.651"	0	0	0
2	80°31'57.502"	28°27'34.726"	8.662	279.240	.224
3	80°31'50.447"	28°27'43.438"	.551	608.936	-.427
4	80°32'21.252"	28°27'39.202"	-590.304	.414	.061
5	80°32'13.149"	28°27'33.769"	-313.591	- .486	.518
6	80°31'55.836"	28°27'22.040"	279.886	- 5.370	.152
7	80°31'46.783"	28°27'15.992"	588.645	- 5.827	-.244
8	80°32'09.514"	28°27'19.496"	29.813	-291.874	.975
9	80°32'16.857"	28°27'11.529"	17.857	-607.976	-.213

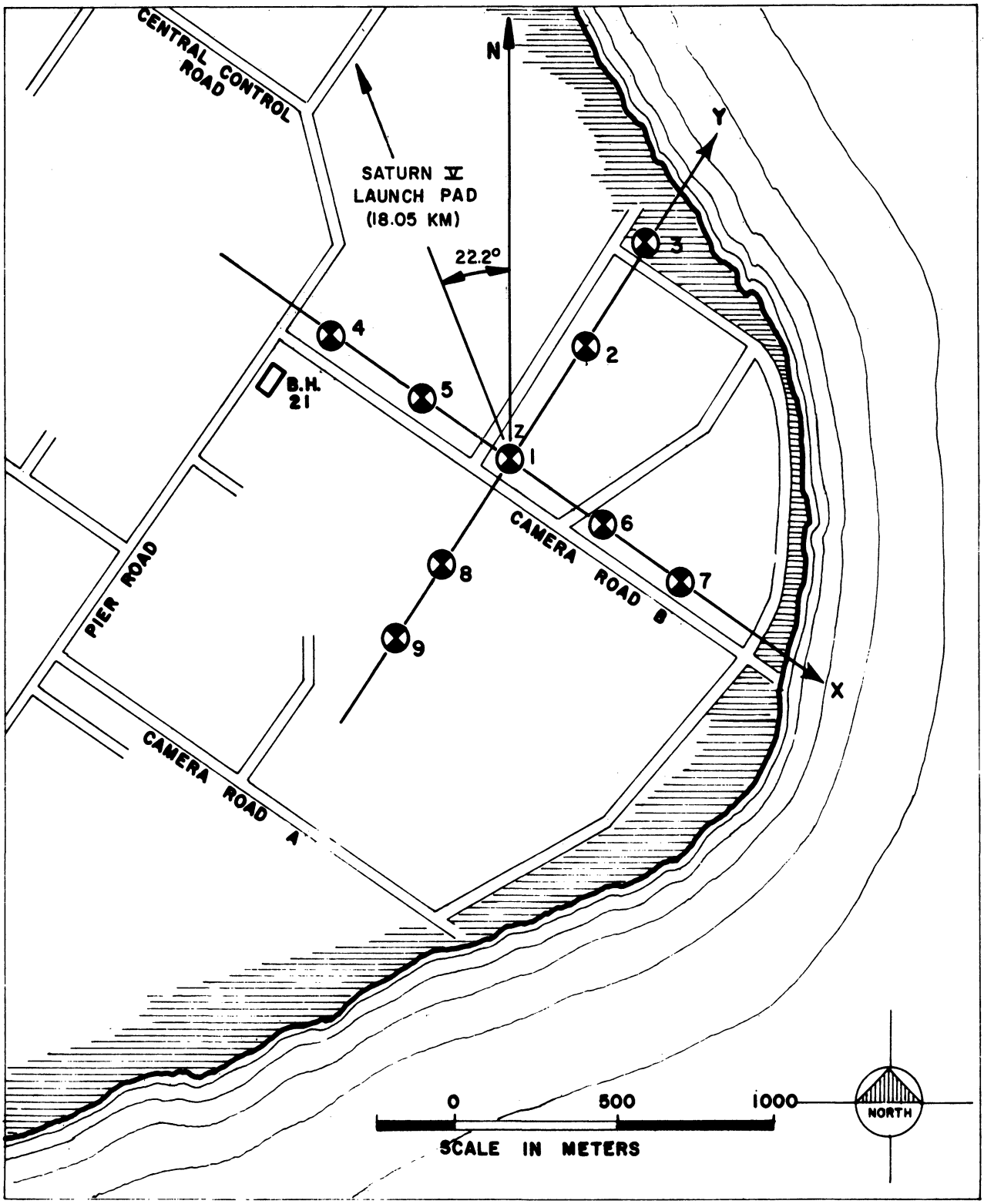

Figure 1. Microphone array.

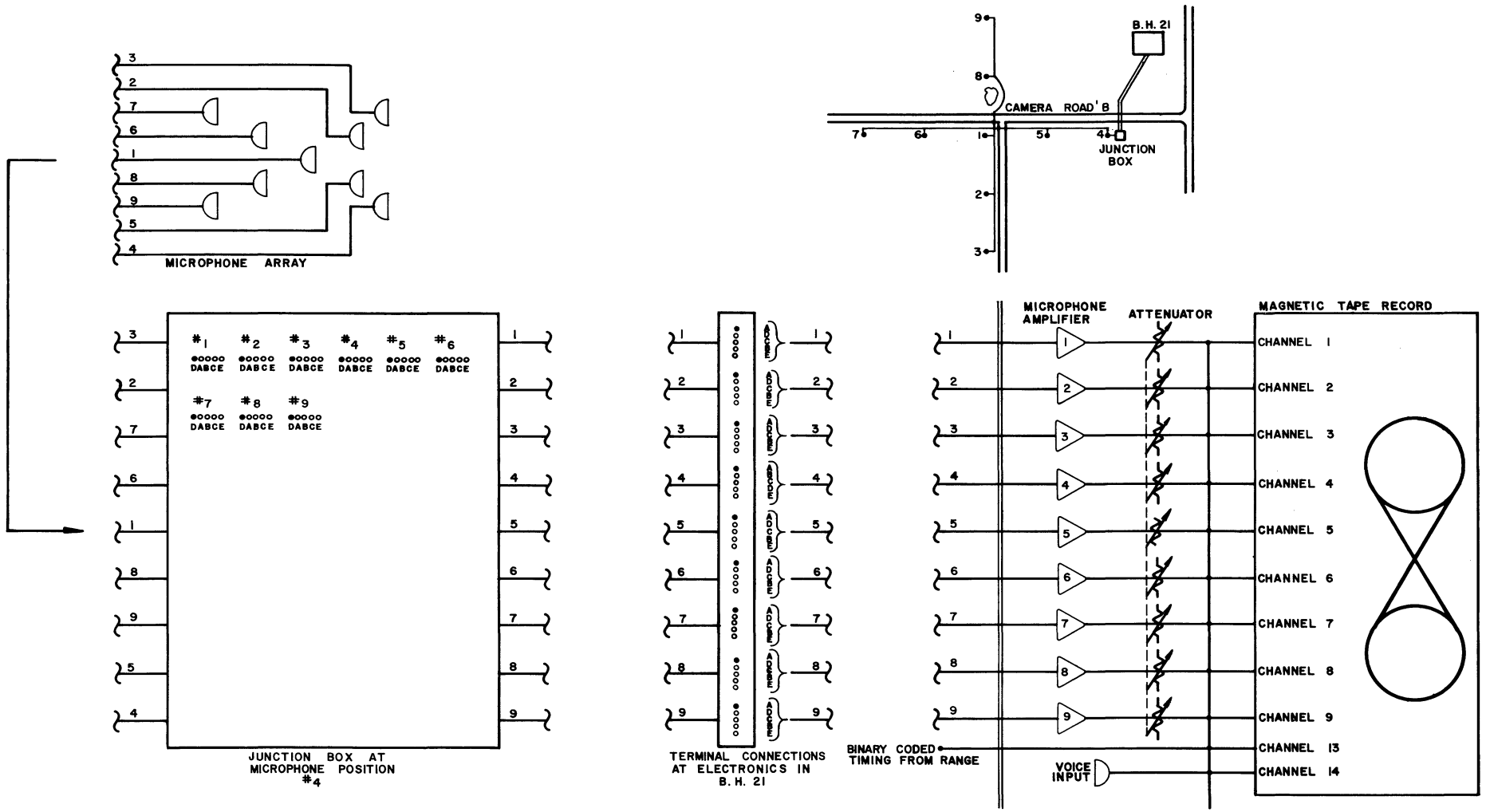

Figure 2. Block diagram of acoustic wind measurement system.

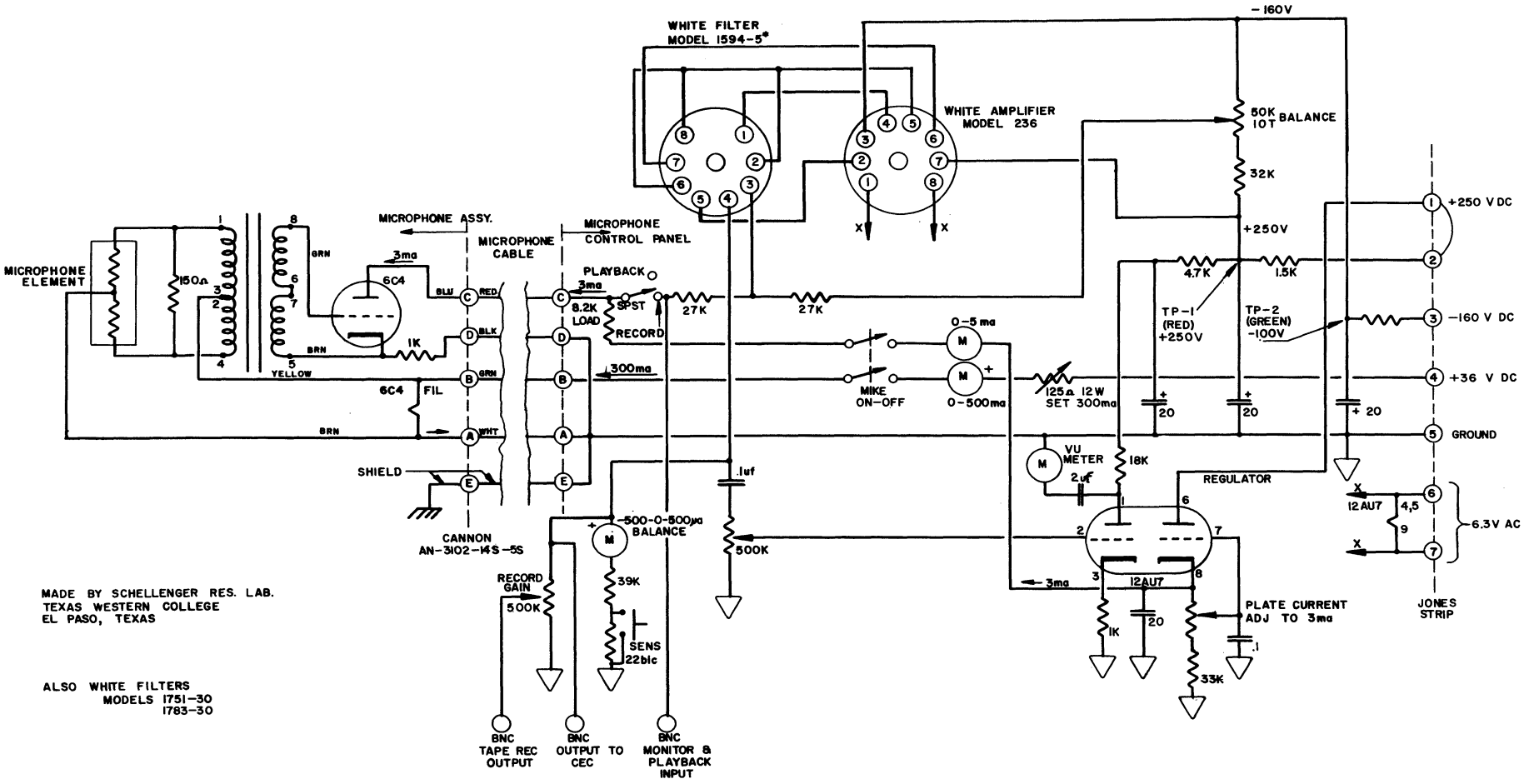

MADE BY SCHELLENGER RES. LAB.
TEXAS WESTERN COLLEGE
EL PASO, TEXAS

ALSO WHITE FILTERS
MODELS 1751-30
1783-30

Figure 3. Hot-wire microphones and control panel.

2.2. REDUCTION OF THE DATA

Since the wavelength of the acoustic disturbance is short compared to the atmospheric scale height, changes in the transmission properties of the atmosphere are generally small. Hence, propagation may be treated by geometric acoustics. The atmosphere is assumed to be horizontally stratified over the range of the experiment. The disturbance travels as a wavefront, and an element of the wavefront will have a velocity which is the sum of the local velocity of the medium and the local speed of propagation in the direction of the wavefront normal.

In the absence of local interference and other absorption effects, the wavefront of a noise event appears essentially the same to each of the separately located microphones. If the characteristics of the microphones used are identical, the output waveform of one microphone matches that of another, except for a time shift. The time shift is a function of the sound arrival angle, the local speed of sound, and the location of the microphone. The time of transit of a sound ray from its source to any given point and its angle of arrival at that point are functions of the temperature and the winds in the layer traversed.

The technique of ray tracing from the ground back to the sound source is well documented in the literature (Bushman, et al., 1965), and will be outlined only briefly in the present report. The assumptions and conditions are that (1) the temperature is determined independently; (2) the vertical component of wind can be ignored; and (3) the plane wave assumption is valid for large distances from the source.

A typical microphone output is shown in Figure 4. Output from three of

the nine microphones is indicated along with the range time. By a method of cross-correlation which is described in detail in Section 2.2.1, the time difference for all microphones from the reference microphone is determined at any point on the record. Since the microphones are placed in a cross-shaped array defining two horizontal axes x and y, the two characteristic velocities K_x and K_y can be calculated. For any noise event, K_x and K_y are constant. Five microphones on both axes permit redundant measurements of these velocities, which are used to minimize random error and to provide first order corrections to the plane wave assumption.

Before the wind can be computed in any layer (the j^{th} in Figure 5), the sound ray is traced through the previous layers where the wind has been calculated. (All the relevant equations are given by Bushman, et al., 1965.) Eventually an interval is reached between the top of the last layer of known wind and the source of the sound. At this point, conventional ray-tracing procedures must be abandoned since the wind is unknown. However, two independent requirements are available: (1) the sound ray must intersect the trajectory, and (2) any intersection will yield a wind value. The correct intersection must satisfy the criterion that the time of arrival of the noise event measured from launch is equal to the time of flight to the intersection plus the time required for the sound to travel from this point to the array. These two conditions uniquely determine the coordination of the source along the trajectory and the average wind in the layer.

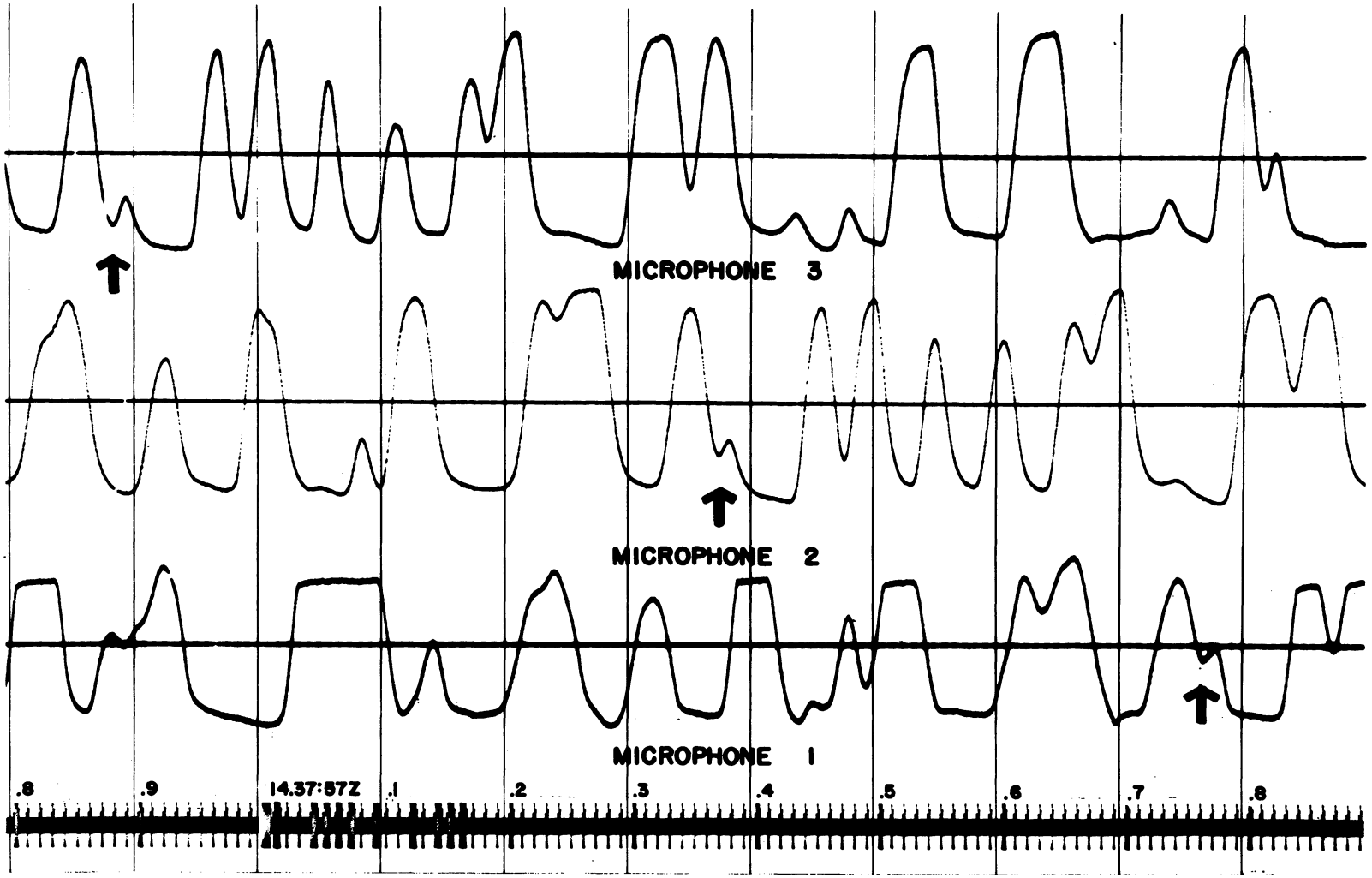

Figure 4. A typical microphone output.

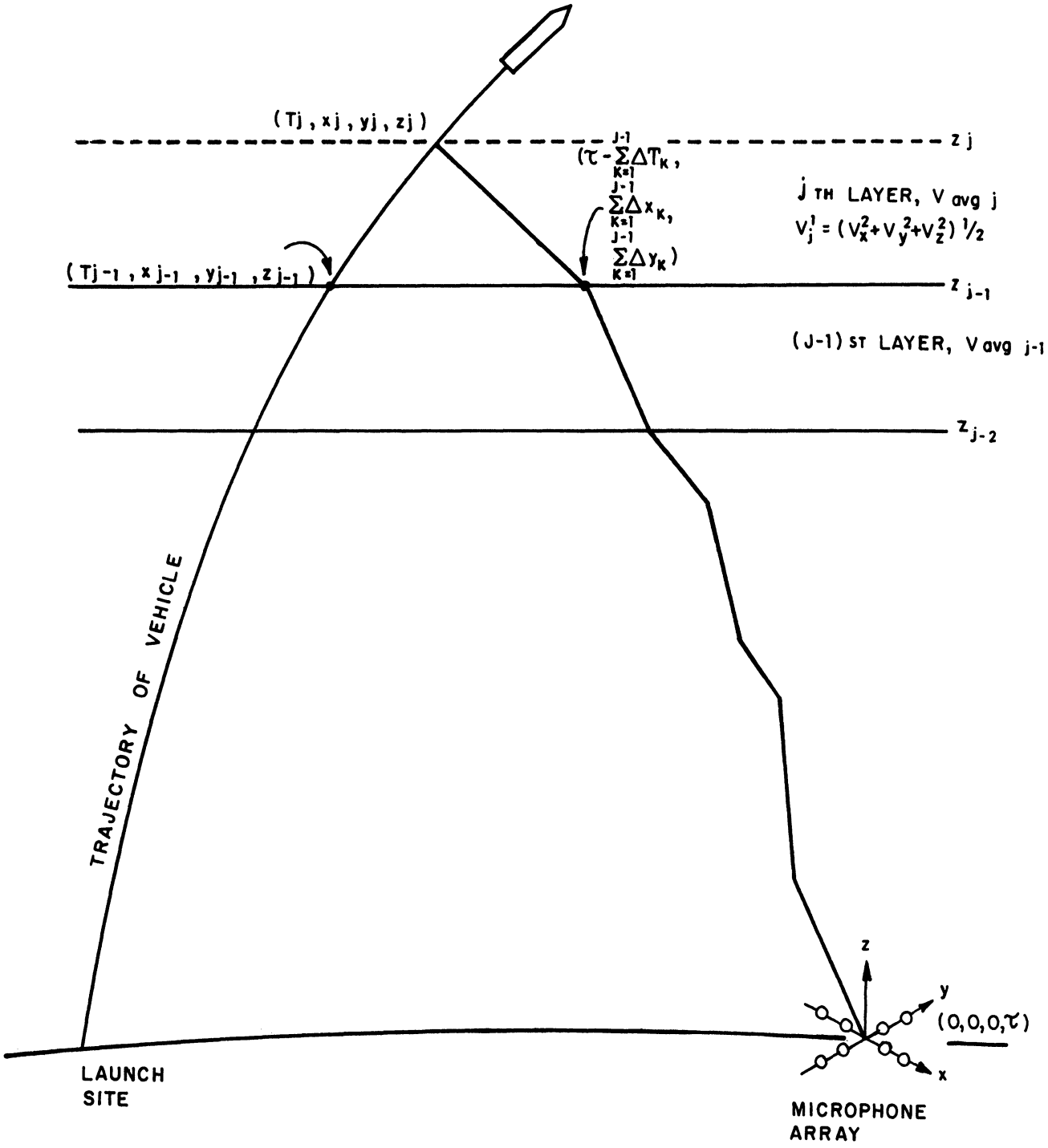

Figure 5. Geometry of the wind experiment showing time relationships for the j^{th} noise event.

2.2.1. Microphone Output Cross-Correlation

Data are received in analog form on magnetic tape, nine channels of microphone data and one channel for range timing. This analog tape is played through an A-D converter and recorded in digital form on another magnetic tape. The present sampling rate is 1000 samples/sec/channel. This number is somewhat arbitrary and was chosen, in this case, to maximize resolution on the computer system currently being used.

Cross-correlation is accomplished using the digital form of the following function:

$$R(t') = \acute{N}\int_{slice} \Psi_1(t)\Psi_2(t+t')dt$$

where R = magnitude of the cross-correlation function,

t' = a variable time difference parameter,

$\acute{N}$ = a normalization factor,

Ψ_1 and Ψ_2 = two time-dependent microphone outputs,

slice = a preset integration time interval.

The computer varies the parameter t' and calculates R for each value. The t' corresponding to the principal maximum of R is the required time difference between the two microphones. The digital equivalent of the cross-correlation function, R, is

$$R = \frac{\sum_{i=1}^{N} x_i y_i - \frac{1}{N}\sum_{i=1}^{N} x_i \sum_{i=1}^{N} y_i}{\left\{\left[\sum_{i=1}^{N} x_i^2 - \frac{1}{N}\left(\sum_{i=1}^{N} x_i\right)^2\right]\left[\sum_{i=1}^{N} y_i^2 - \frac{1}{N}\left(\sum_{i=1}^{N} y_i\right)^2\right]\right\}^{1/2}}$$

where x_i and y_i represent samples of individual microphone outputs and N is the number of sample pairs.

These computations are performed for a preset data time interval (slice), usually 0.5 sec, which makes N equal to 500 sample pairs/slice. Occasionally a microphone will not yield a good correlation during a particular slice. This is usually caused by switching transients, changing attenuation of the incoming signal, background noise, or wind interference. The computer version of the cross-correlation computation follows.

PROBLEM: Given a time series

$$x(t)\left[t_o - \frac{a}{2} \leq t \leq t_o + \frac{a}{2}\right]$$

for the reference microphone and a time series

$$y(t)\left[t_o - \frac{a}{2} + t'_a - \epsilon \leq t \leq t_o + \frac{a}{2} + t'_a + \epsilon\right]$$

and the t'_o which maximizes the R is given by:

$$R^2(t') = \frac{\left\{\left[N\sum_{t=t_o-\frac{a}{2}}^{t_o+\frac{a}{2}} x(t)y(t+t')\right] - \left[\sum_{t=t_o-\frac{a}{2}}^{t_o+\frac{a}{2}} x(t)\right]\left[\sum_{t=t_o-\frac{a}{2}}^{t_o+\frac{a}{2}} y(t+t')\right]\right\}^2}{\left\{N\Sigma[x(t)]^2 - [\Sigma x(t)]^2\right\}\left\{N\Sigma[y(t)]^2 - [\Sigma y(t)]^2\right\}}$$

where N is the number of points of the time series in the interval

$$\left(t_o - \frac{a}{2}, \quad t_o + \frac{a}{2}\right)$$

and t' ranges over

$$(t'_a-\epsilon \ , \quad t'_a+\epsilon)$$

If $R_o > .7$ then R_o is considered a significant peak.

INTERPOLATION: A cost-saving option of this program is to read every k^{th} point off the tape instead of every point. The resolution of the result t'_o is thus reduced by a factor of k, but this resolution is improved by performing a second-order interpolation on the points (t'_{-1}, R_{-1}), (t'_o, R_o), (t'_1, R_1) where $t'_1 = t'_o+k$, and $t'_{-1} = t'_o-k$. It has been found that if the sampling frequency of the tape is 1000 samples/sec and if k = 5, the interpolation procedure will provide t'_o with a resolution very close to 1 msec and the cost of running the program is cut by a factor of 5.

INPUT PARAMETERS FOR CROSS-CORRELATION PROGRAM

a	window
ϵ	tolerance
t'_a	table of estimates for t_o given at selected times during the flight
k	equals 2, 3, 4, etc. depending upon whether every 2nd point is to be read from input tape or every 3rd, every 4th, etc.
SF	sampling frequency of the tape
$t_{o\ min}$	start time
$t_{o\ max}$	stop time
Δt_o	increment for t_o
n	number of microphones to be compared with reference microphone

COMPUTER INPUT DATA FOR CROSS-CORRELATION PROGRAM

1. $t_{o\ min}$, $t_{o\ max}$, Δt_o, a, ϵ; FORMAT (5F8.4)

2. n, M, REFERENCE MIC, ROW, k; FORMAT (3I1, 2I3)

3. FILE, SF, HOUR, MIN, SEC; FORMAT (I1, F4.1, 2I2, F7.3)

4. MIC_1, MIC_2,.....,MIC_n; FORMAT (9I1)

5. t'_a table of the form:

.

. time mic_1 mic_2 mic_3.....mic_9; FORMAT (10F8.4)

.

.

5+ROW

where

n number of microphones on tape (including the reference microphone)

REFERENCE MIC number of the reference microphone

ROW number of cards containing t'_a table

FILE file number on tape where time series are found

HOUR, MIN, SEC } reference time of the flight

MIC_j number of the j^{th} microphone to be compared with the reference microphone. For example, if microphones 8, 9, 4, 2, are to be compared (in that order) with the reference microphone, then card 4 would read: 8942

mic_j estimate of t'_o for microphone number j at the time given on the first field of the card.

Figure 6 shows the variation of the cross-correlation coefficient with the time difference for a typical microphone pair. Figure 7 gives the general flow of the program and Figure 8 gives the algorithm for finding t_o'. All time parameters are given in seconds after reference time.

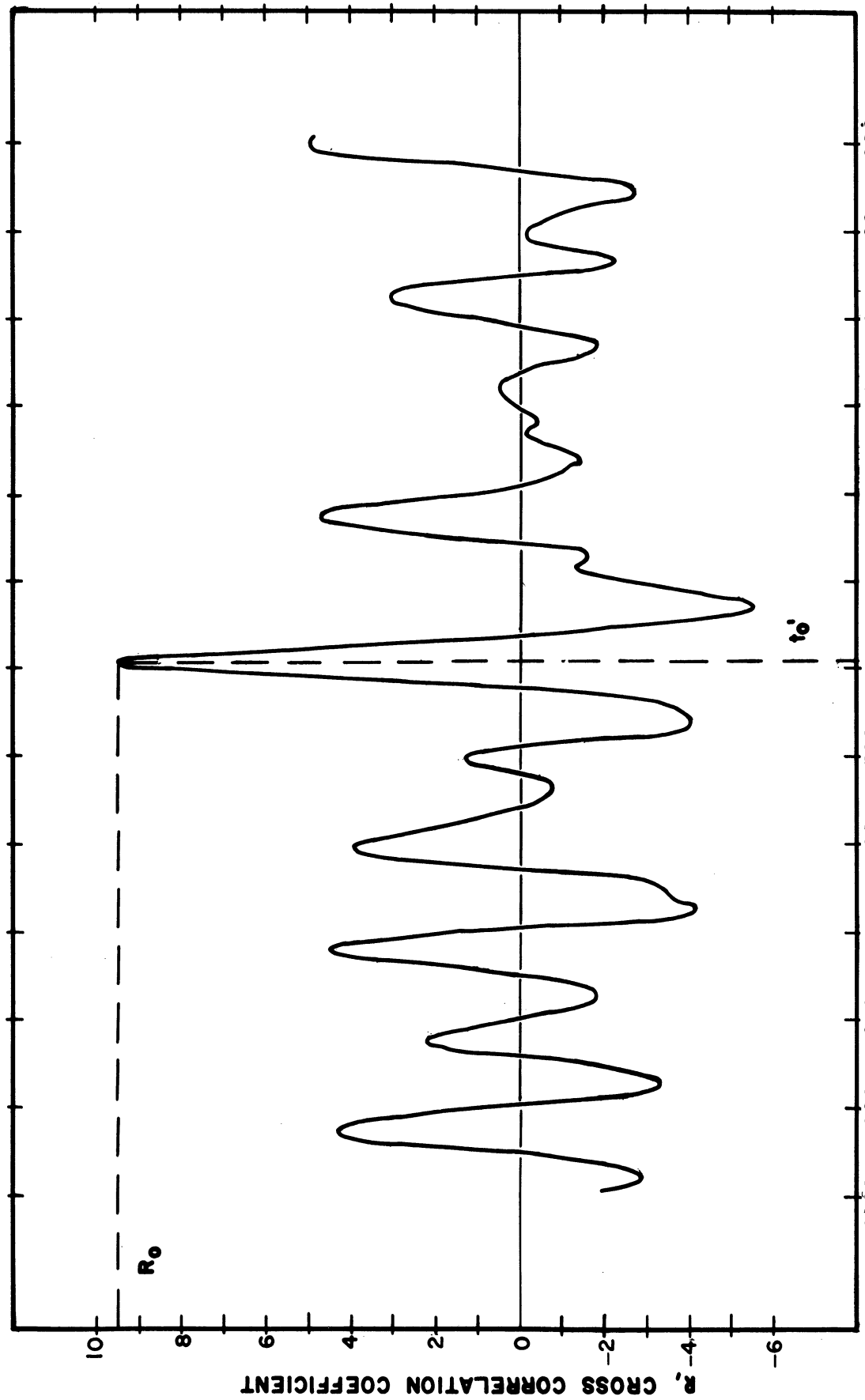

Figure 6. Variation of cross-correlation coefficient with time difference for a typical microphone pair.

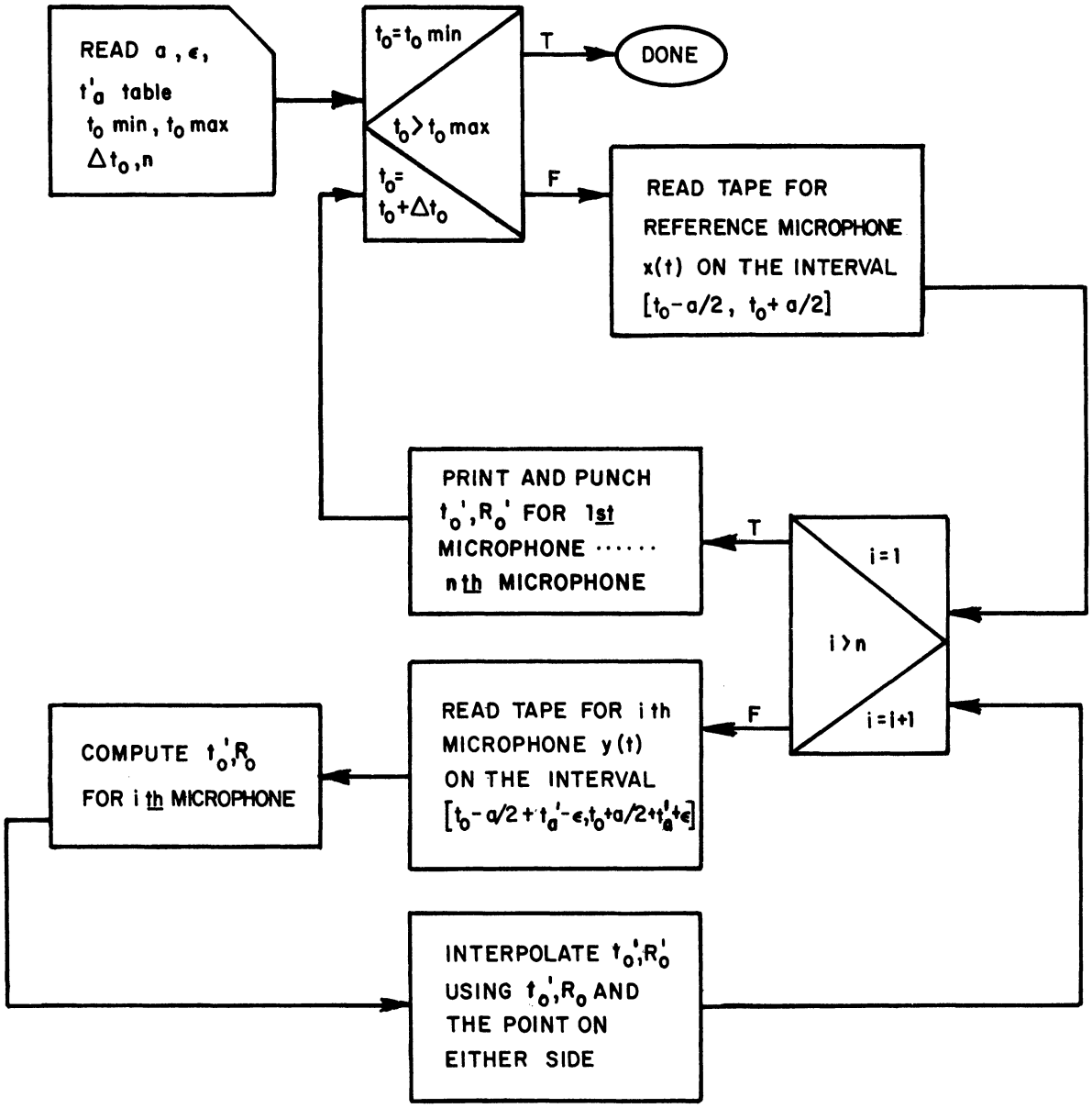

Figure 7. General flow of the cross-correlation program.

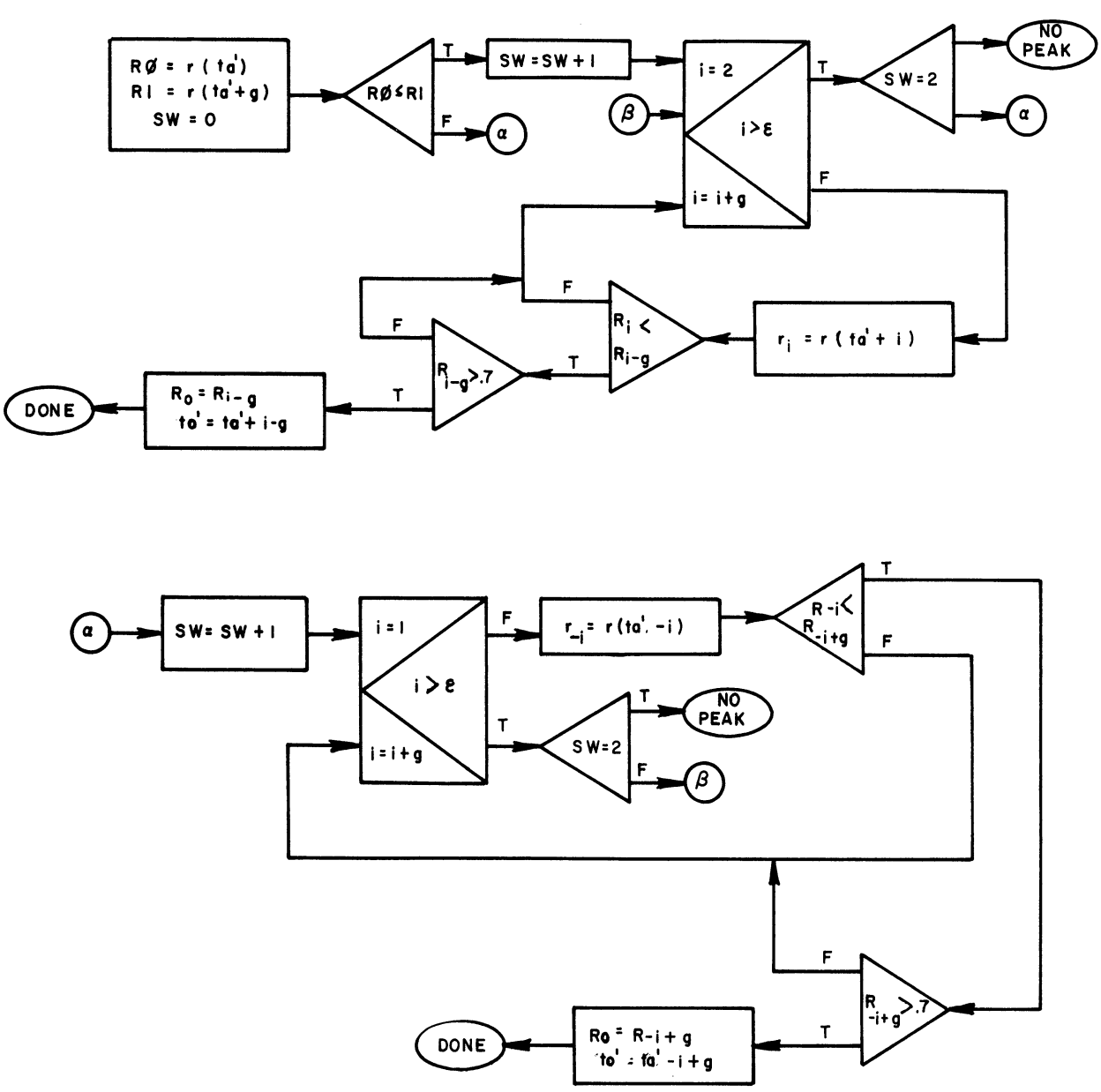

Figure 8. Algorithm for finding t'_o.

2.2.2. Wind Computation

The solution for winds has been programmed for the IBM 360/67 computer in Fortran IV language. Figure 9 shows the flow diagram for the wind computation.

The temperature profile (or the equivalent speed of sound profile) is obtained from radiosonde and rocketsonde measurements up to about 60 km. Above that altitude the temperature is obtained from the Patrick AFB Reference Atmosphere (Smith and Weidner, 1964). For the computer input the temperature profile is piecewise linearized into a number of straight line segments corresponding to layer thickness,

$$V = cZ + d$$

where c and d are coefficients for the segment corresponding to the altitude Z.

The average speed of sound for the j^{th} layer, V_{avg_j}, is defined as

$$V_{avg_j} = \frac{1}{(Z_j - Z_{j-1})} \int_{j-1}^{Z_j} V(\acute{Z}) d\acute{Z}$$

where the top of the layer is at Z_j and the bottom at Z_{j-1}. The vehicle positional data are known at half-second intervals. These data are corrected for the position of the noise source, which is considered to be a point located at the nozzle of the engine or at a known distance behind the nozzle along the flight path.

Let $\acute{X}$, $\acute{Y}$, and $\acute{Z}$ be the given position at the time T (the reference point is generally the center of gravity of the rocket). The coordinates of the noise source X, Y, Z, are

$$X = \acute{X} - \frac{\Delta R \frac{d\acute{X}}{dT}}{\sqrt{\left(\frac{d\acute{X}}{dT}\right)^2 + \left(\frac{d\acute{Y}}{dT}\right)^2 + \left(\frac{d\acute{Z}}{dT}\right)^2}}$$

and similarly for Y and Z. ΔR is the estimated distance between the center of gravity of the rocket and the noise source (Dyer, 1959).

For the j^{th} noise event, the sound is heard at the time τ from lift-off at the microphone array and the characteristic velocities K_x and K_y are determined. The characteristic velocities are defined as the velocities of interaction of the wavefront with the X and Y axes. Before the wind can be computed in any layer (the j^{th}), the sound ray is traced through the previous layers where the wind has been found. The components of the sound velocity of the j^{th} noise event in any previous layer (the i^{th}) are

$$V_{x_i} = \frac{V^2_{avg_i}}{K_{x_j} - W_{x_i} - W_{y_i}\left(K_{x_j}/K_{y_j}\right)},$$

$$V_{y_i} = V_{x_i} \frac{K_{x_j}}{K_{y_j}},$$

$$V_{z_i} = \left(V^2_{avg_i} - V^2_{x_i} - V^2_{y_i}\right)^{1/2}.$$

The coordinates of the point of penetration at Z_{j-1} (Figure 5) can then be calculated:

$$\sum_{K=1}^{j-1} \Delta t_K, \quad \sum_{K=1}^{j-1} \Delta X_K, \quad \sum_{K=1}^{j-1} \Delta Y_K.$$

In order to calculate the wind in the top layer, a reasonable value for T_j must be selected, based upon the velocity of sound and winds in the lower layers. This value determines the coordinates X_j, Y_j, and Z_j along the trajectory, and the three components of the speed of sound V_x, V_y, and V_z in the top layer. The criterion for choosing T_j correctly is that the average value of the speed of sound in the top layer thus calculated should agree with the value derived from the given speed of sound profile. In this way the true position of sound emittance is found and the wind in the top layer is determined:

$$\vec{W} = \vec{P} - \vec{V} \qquad \text{(Bushman, } \underline{\text{et}} \text{ } \underline{\text{al}}\text{., 1965)}$$

where $\vec{W}$ is the wind vector, $\vec{P}$ is the propagation velocity vector, and $\vec{V}$ is the velocity of sound vector.

Instead of estimating the time of the j^{th} noise event measured along the trajectory of the vehicle (T_j), it is easier to estimate δT_j (equal to $T_j - T_{j-1}$). Initial estimates of δT_j need be only very approximate for the convergence of the solution. The better these estimates, the less time the computations will take. Newton's method of solving equations is used for fast convergence rather than using small increments in T_j.

$$T_j = T'_j - \frac{f(T'_j)}{f'(T'_j)}$$

where T'_j = assumed value,

$f(T'_j)$ = value of given function at T'_j,

$f'(T'_j)$ = value of first derivative of function at T'_j,

T_j = second approximation to the root.

T_j may be substituted for T'_j in this formula to obtain a third approximation to the root. A tolerance of about one m/sec between v_j and $v_{avg_j}(\epsilon_1)$ is acceptable.

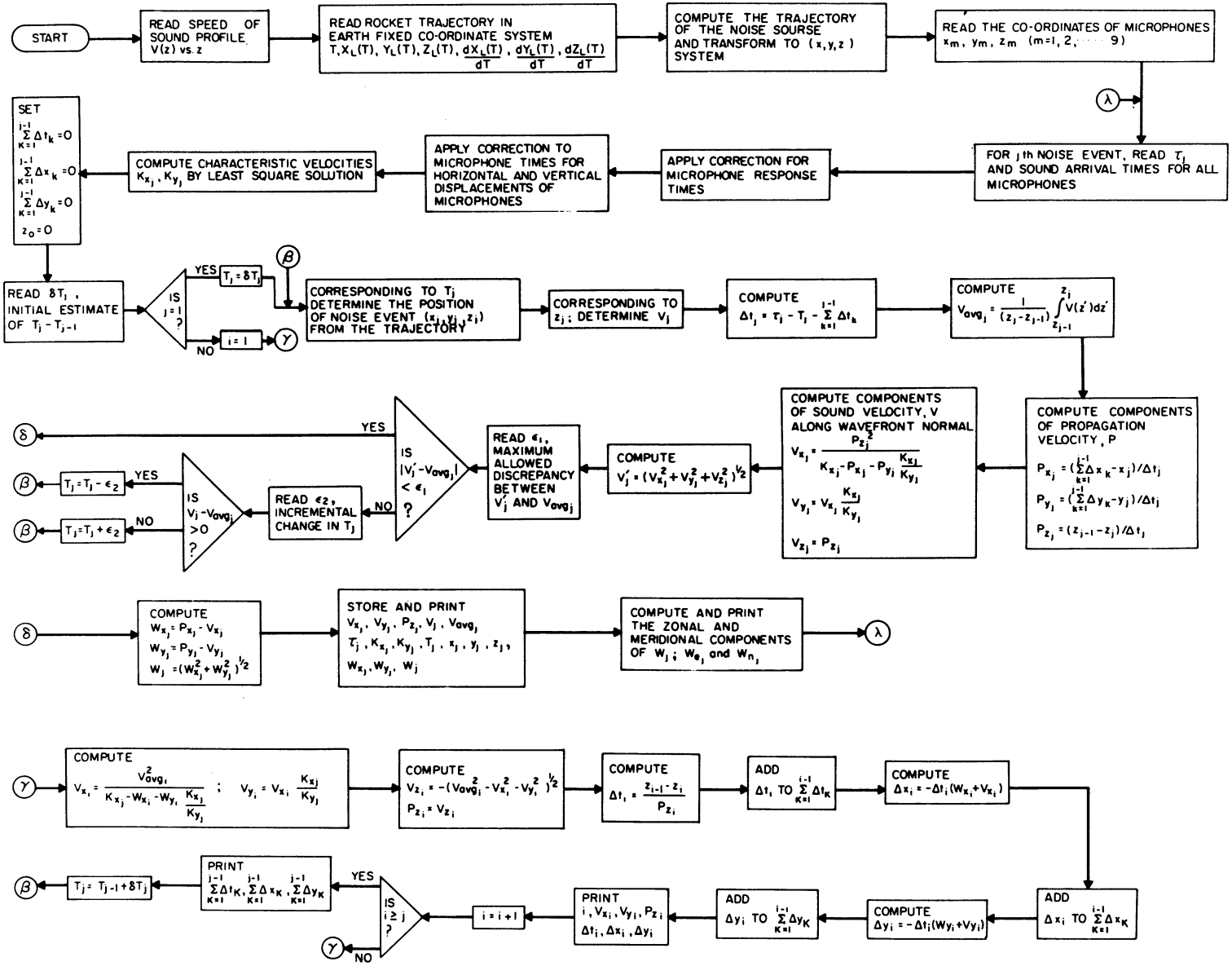

Figure 9. Flow diagram for wind computation.

3. WIND PROFILES

Wind profiles have been generated for all Apollo (Saturn) Series launches, as well as for flights of Atlas Agena C, Titan IIIC-5, and Thor Delta 63. Some wind profiles for the Apollo (Saturn) do not extend as high as 85 km because the trajectory becomes quite flat above 60-65 km and the data are no longer useable. The profiles of the Thor and the Atlas class vehicles are as good as those of the Saturn vehicles and, in some cases, even better because of the more vertical trajectory common to the smaller class rockets.

Acoustic wind measurements have been made for a total of 19 rocket firings (see Table II). The first of these measurements was for the Saturn (SA-6), the first Apollo Flight Model, launched on 29 May 1964, which is not shown in Table II. Only three microphones were used in this flight and their sites were not accurately surveyed. The purpose of the SA-6 launch measurements was to test the microphone performance and to determine whether the exhaust noise recordings for different microphones could be cross-correlated and meaningfully interpreted. The data were significant, but the wind measurements derived from this launch were questionable because of the lack of redundancy in the measurement and because of survey errors.

The first successful attempt to derive a wind profile was for the SA-9 launch. Data from all subsequent flights have been analyzed except for the Minuteman and Titan IIIC-5 flights. In the case of the Minuteman flight, no trajectory information was available. For the Titan IIIC-5, the range times could not be read from the magnetic tape, and analysis of the data was not

possible. A strip chart recording of this flight will be made to determine the reason for the difficulty.

In all the rocket flights, analysis of the data was made up to the altitudes of the first stage burnout. For the SA- Series firings, the trajectory was relatively steep and the staging occurred at an altitude of 85 km and a slant distance of about 106 km. In the case of the AS- Series firings, the trajectory was flatter, the staging altitude was about 63 km, and the slant distance was about 110 km. The wind profiles in Figures 10-25 show that the wind determination was carried out to higher altitudes for the SA- Series than for the AS- Series. Whenever rawinsonde and rocketsonde measurements taken at approximately the same time as the rocket launch were available, they were included on the figures.

TABLE II

ROCKET LAUNCH DATA

Flight	Date	Time (GMT)	Launch Complex	Firing Direction	Distance to Mic. #1 (km)	Ground Temperature (°K)	Ground Wind Speed (m/sec)
SA-9	2-16-65	14:37:03	37B	105°	8.75	296.3	4.8
Ranger 8	2-17-65	17:05:01	12	95°	2.66	298.9	6.0
SA-8	5-25-65	07:35:01	37B	105°	8.75	296.0	4.5
SA-10	7-30-65	13:00:00	37B	95°	8.75	297.7	13.6
AS-201	2-26-66	16:12:01	34	105°	7.59	288.6	6.0
AS-203	7- 5-66	14:53:17	37B	72°	8.75	302.7	8.5
AS-202	8-25-66	17:15:32	34	105°	7.59	302.6	2.5
Titan IIIC	8-26-66	13:59:56	41	90°	14.70	*	*
Atlas Agena	11- 5-67	23:37:00	12	90°	2.66	*	*
Minuteman	11- 6-67	00:56:00	*	*	*	*	*
AS-501	11- 9-67	12:00:01	39A	72°	18.05	285.6	9.0
AS-204	1-22-68	22:48:08	37B	72°	8.75	289.1	2.0
AS-502	4- 4-68	12:00:01	39A	72°	18.05	292.6	8.0
Titan IIIC-5	9-28-68	07:37:00	41	93°	14.70	*	*
AS-205	10-11-68	15:02:45	34	72°	7.59	300.95	8.0
Delta 63	12-19-68	00:32:00	17A	100°	3.45	289.5	*
AS-503	12-21-68	12:51:00	39A	72°	18.05	288.0	1.0
AS-504	3- 3-69	16:00:00	39A	72°	18.05	285.95	3.0

*Not available

	Mic. #1	Complex 12	Complex 17A	Complex 34	Complex 37B	Complex 39A	Complex 41
Long. (W)	80.534426	80.542495	80.565203	80.561141	80.564953	80.604133	80.5831045
Lat. (N)	28.457681	28.480745	28.446875	28.521963	28.531854	28.608422	28.5831770

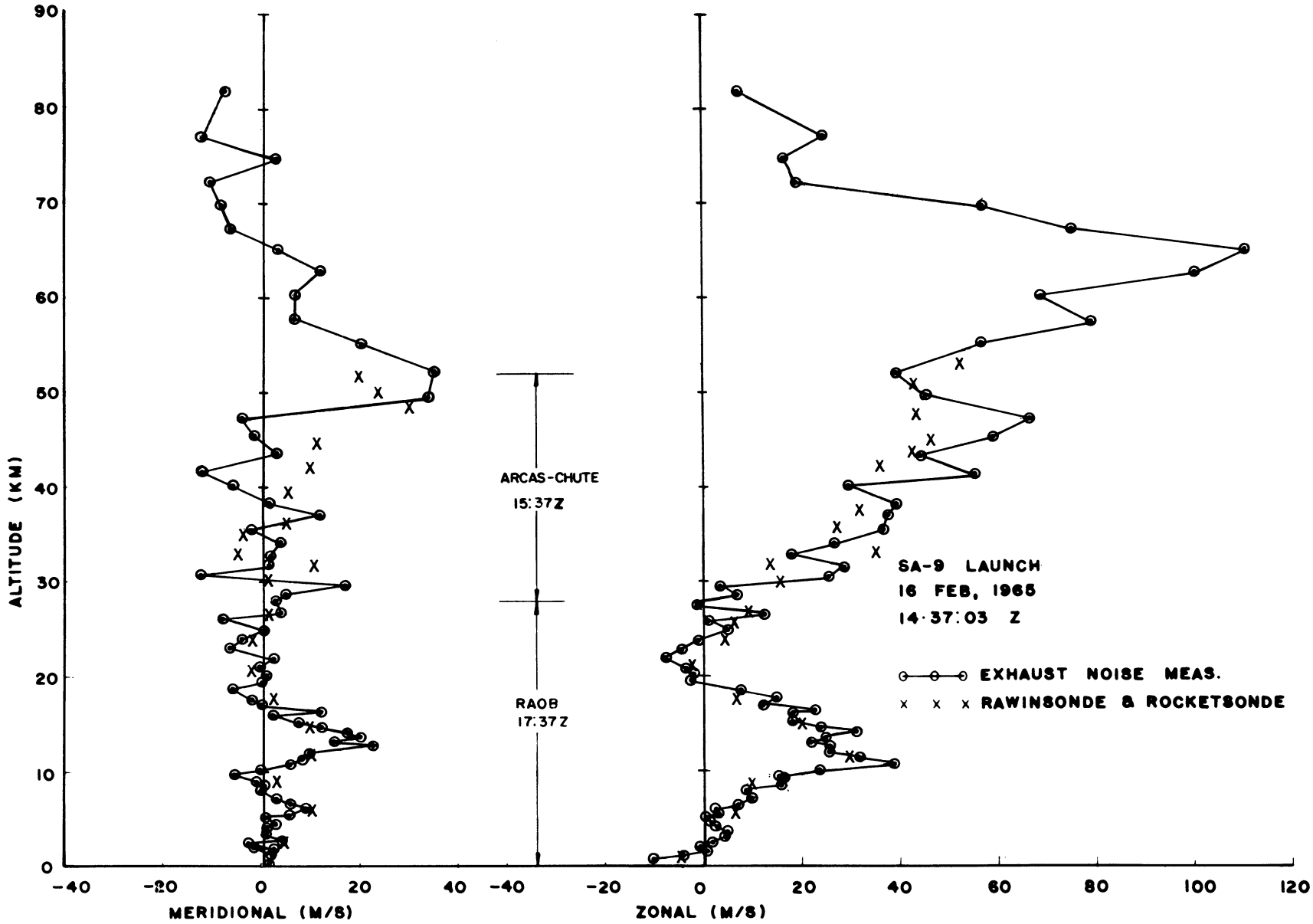

Figure 10. Wind profile, SA-9, 16 February 1965.

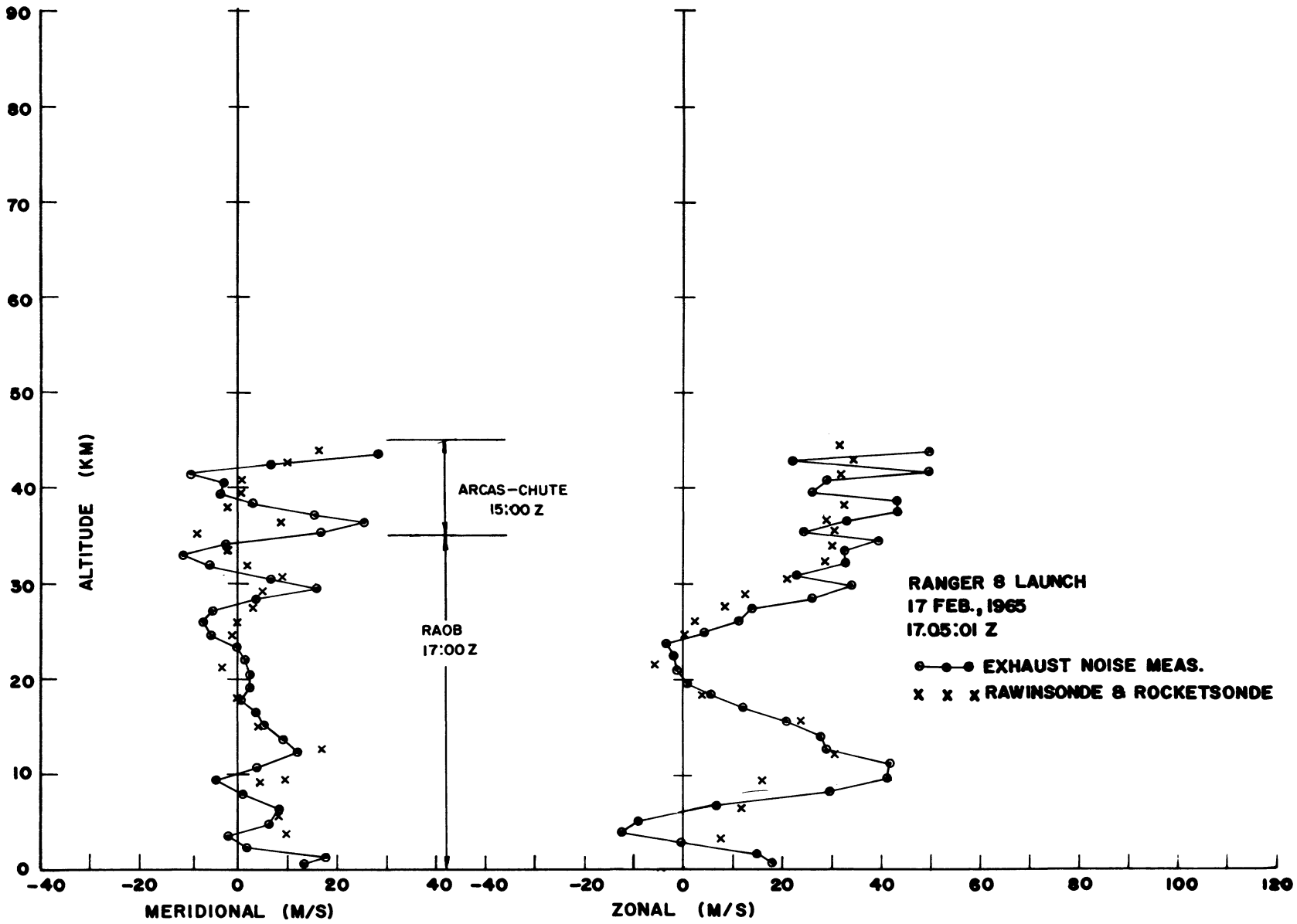

Figure 11. Wind profile, Ranger 8, 17 February 1965.

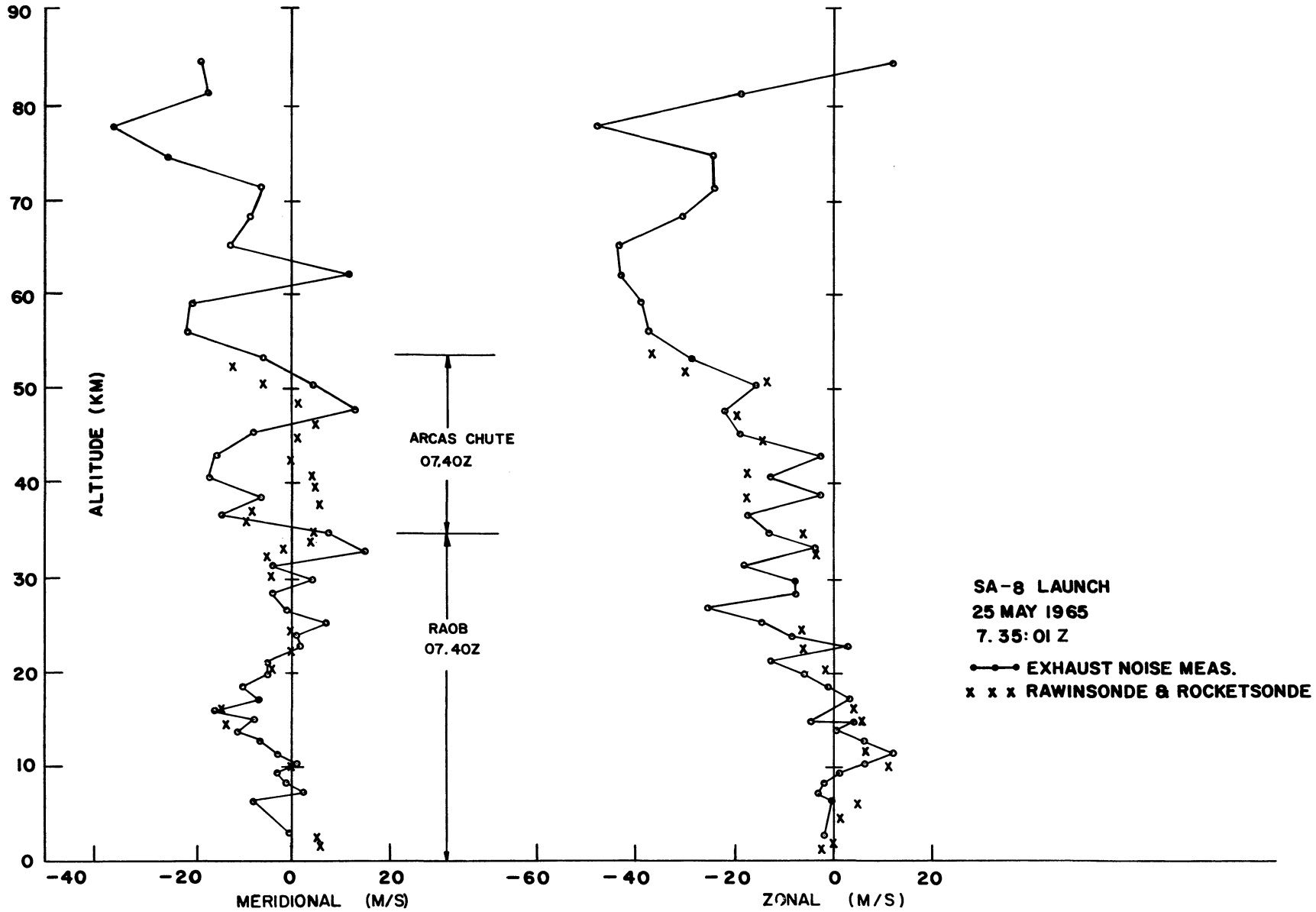

Figure 12. Wind profile, SA-8, 25 May 1965.

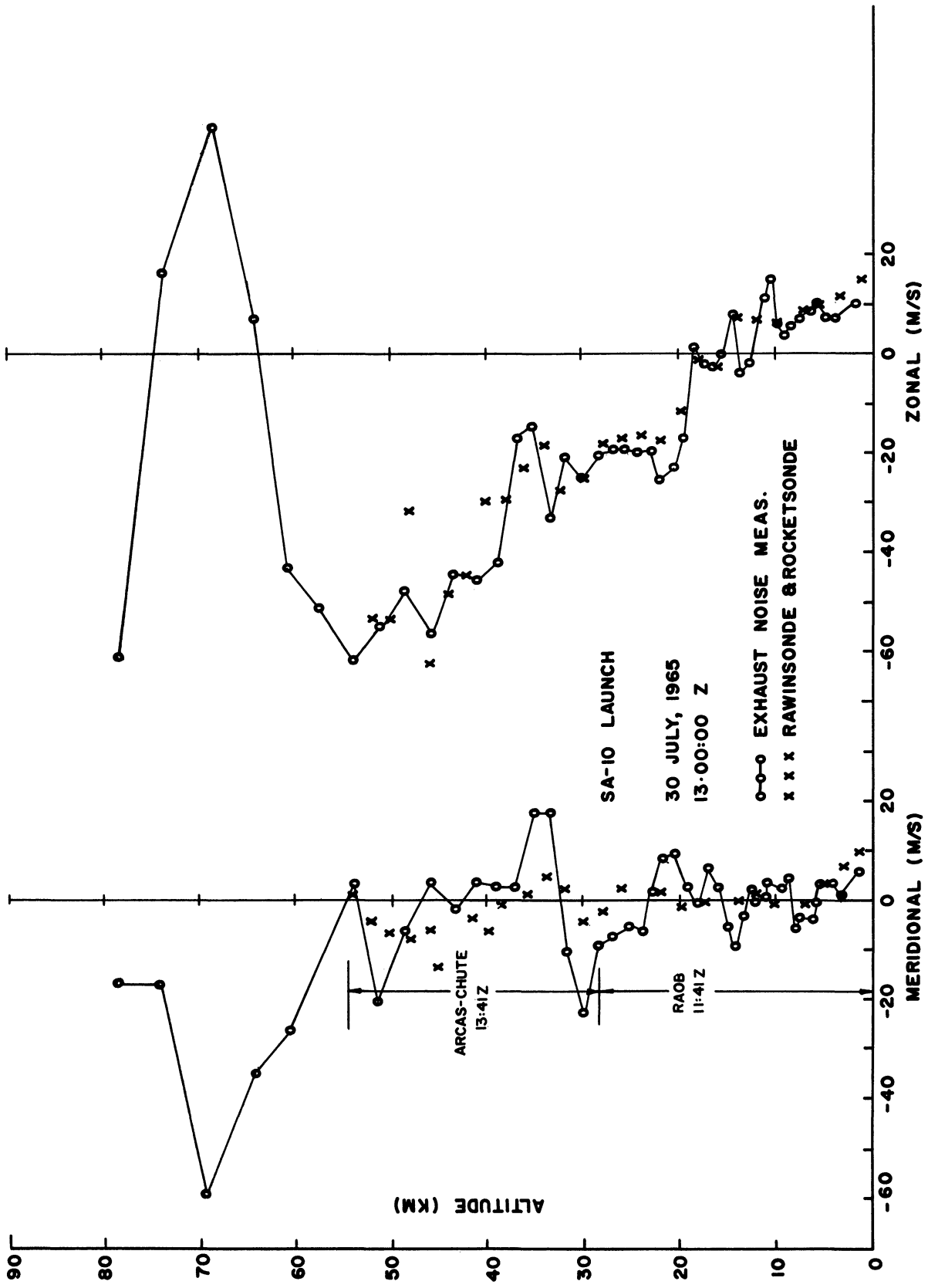

Figure 13. Wind profile, SA-10, 30 July 1965.

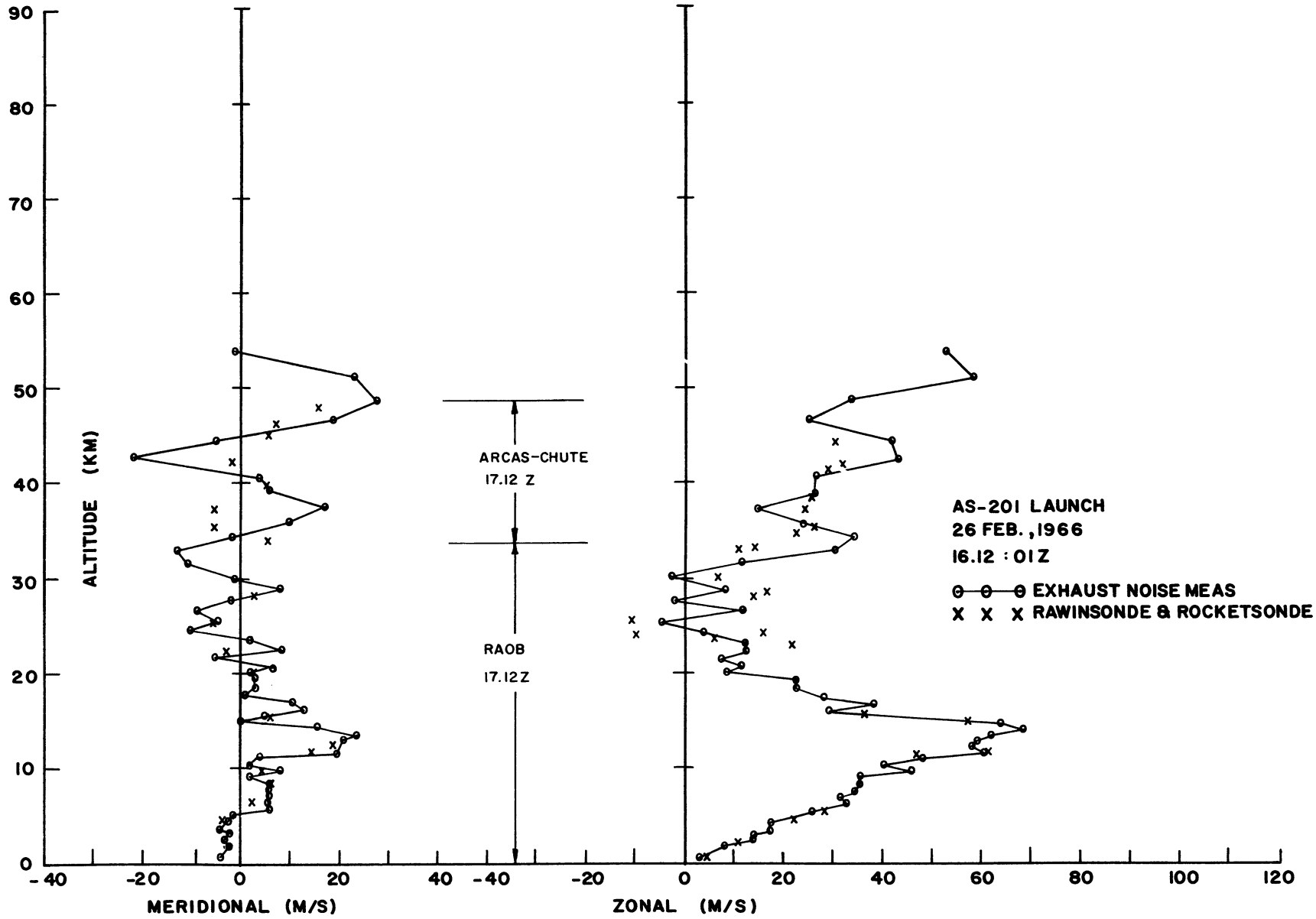

Figure 14. Wind profile, AS-201, 26 February 1966.

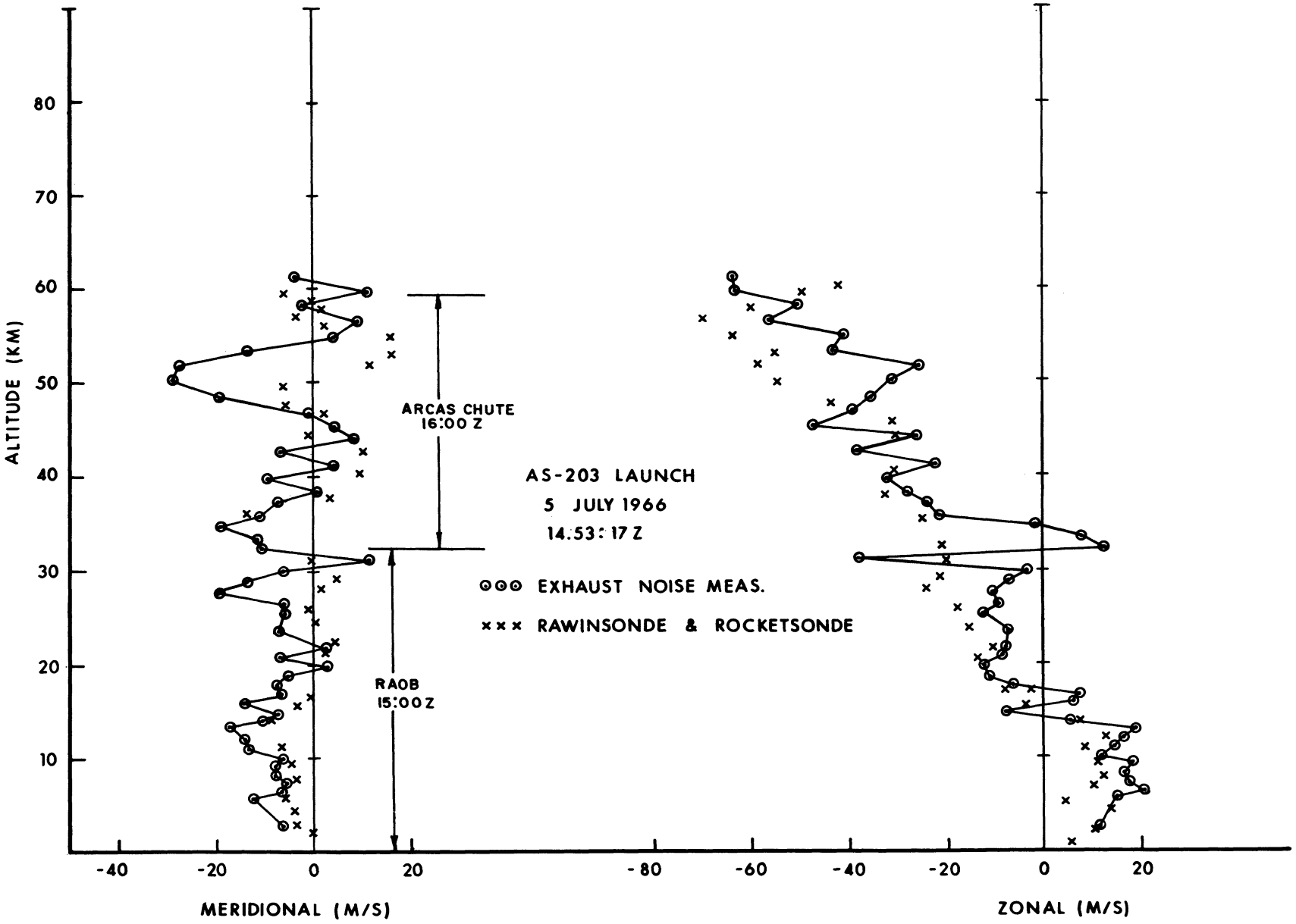

Figure 15. Wind profile, AS-203, 5 July 1966.

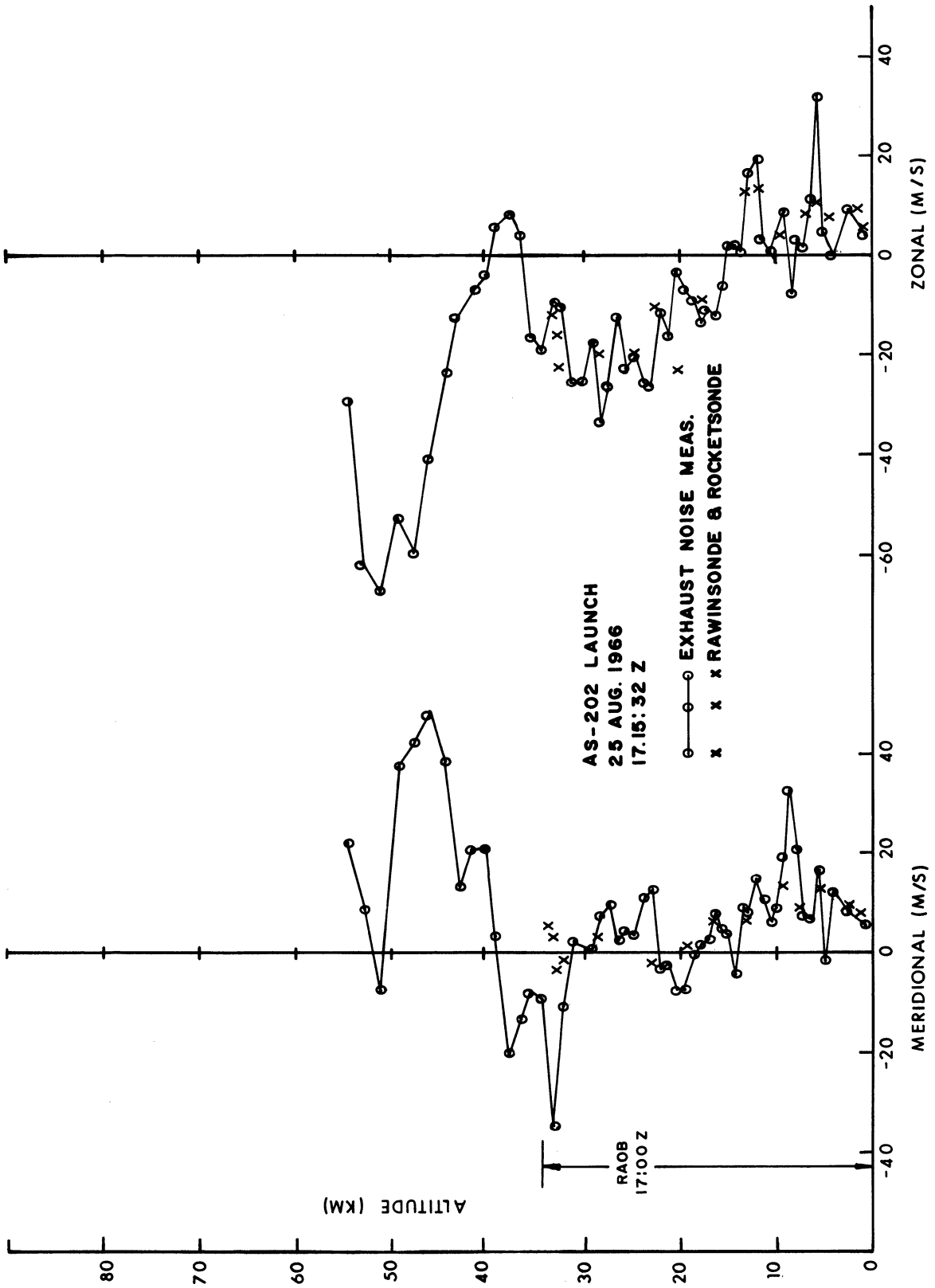

Figure 16. Wind profile, AS-202, 25 August 1966.

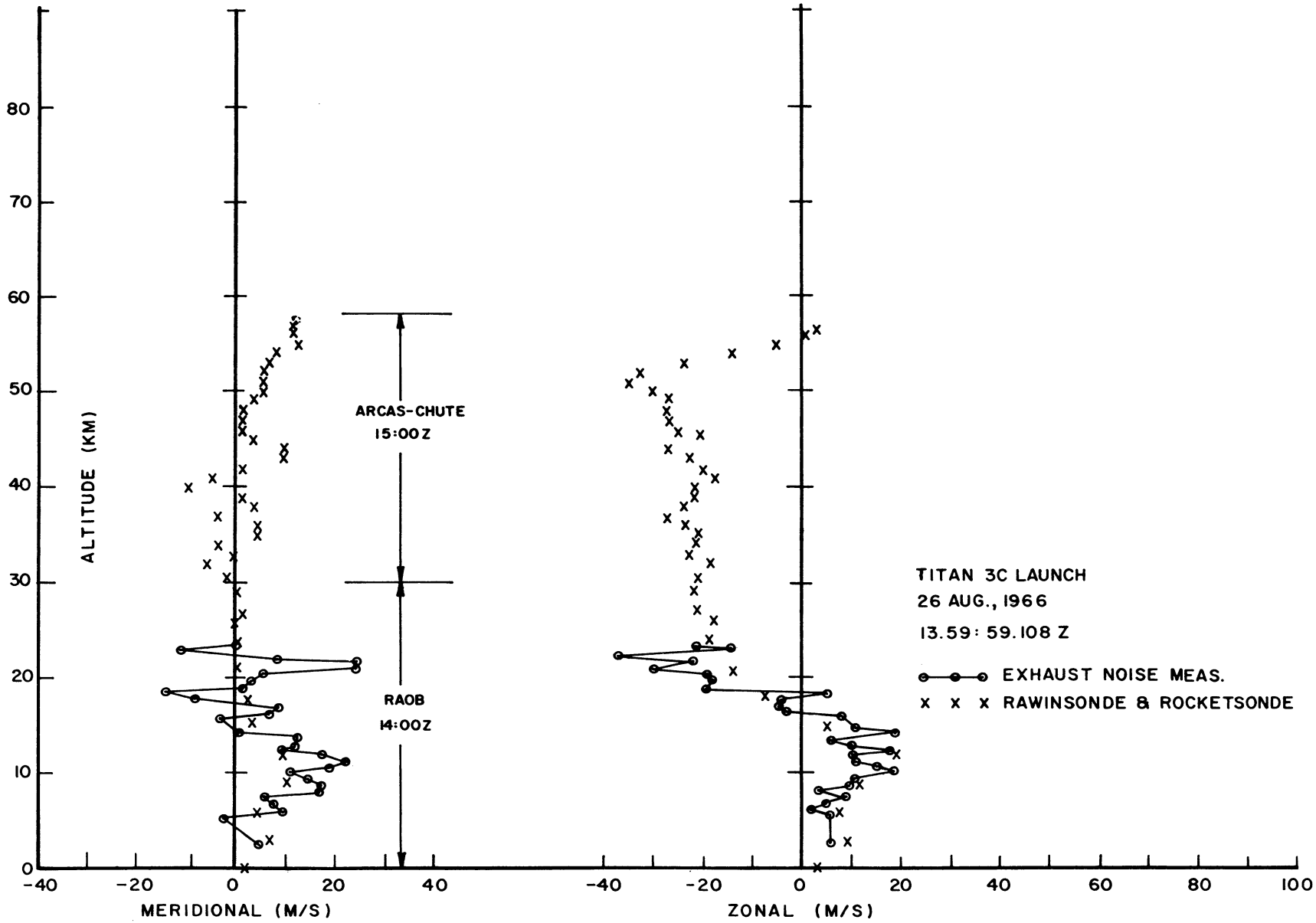

Figure 17. Wind profile, Titan IIIC, 26 August 1966.

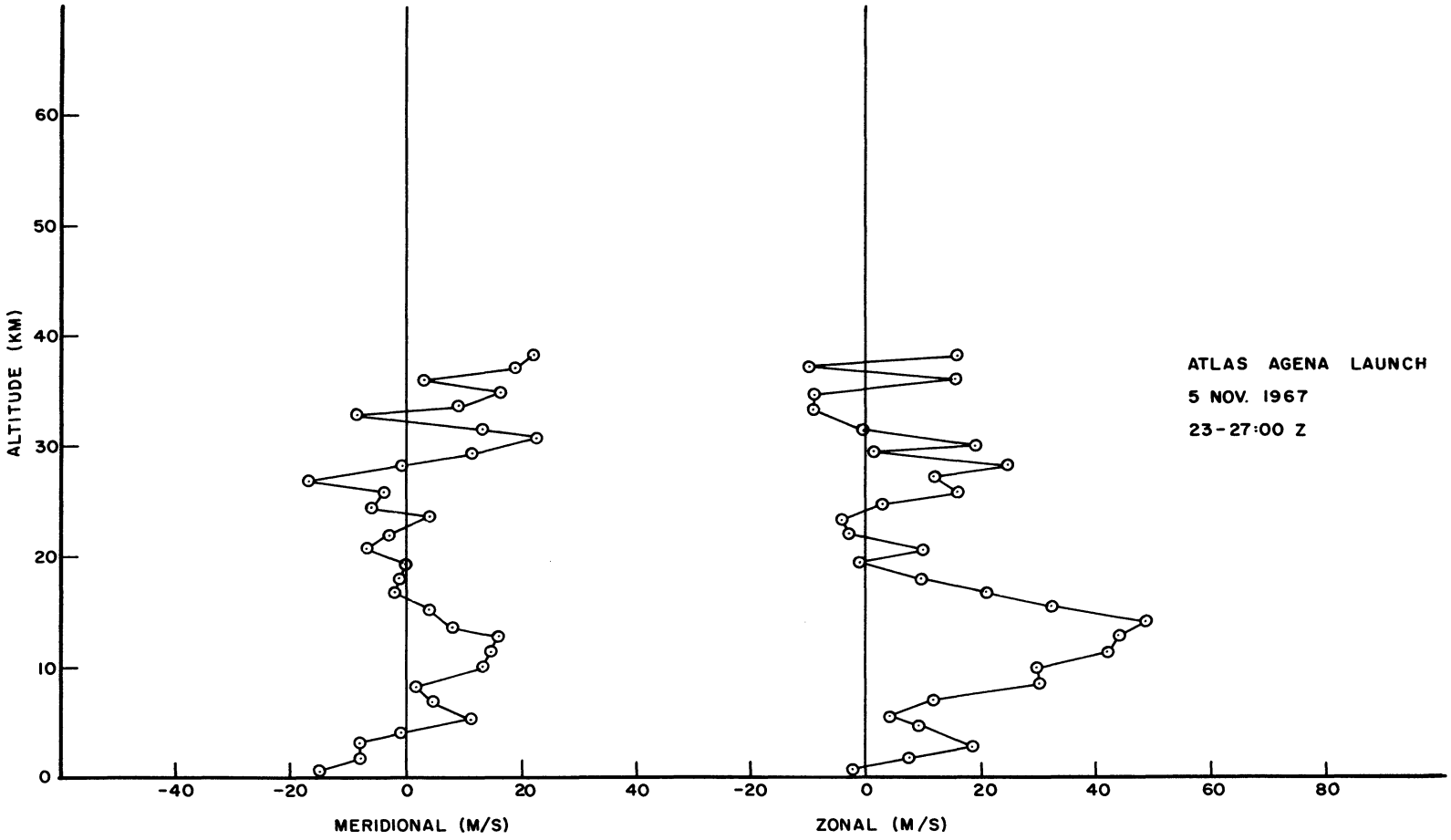

Figure 18. Wind profile, Atlas Agena, 5 November 1967.

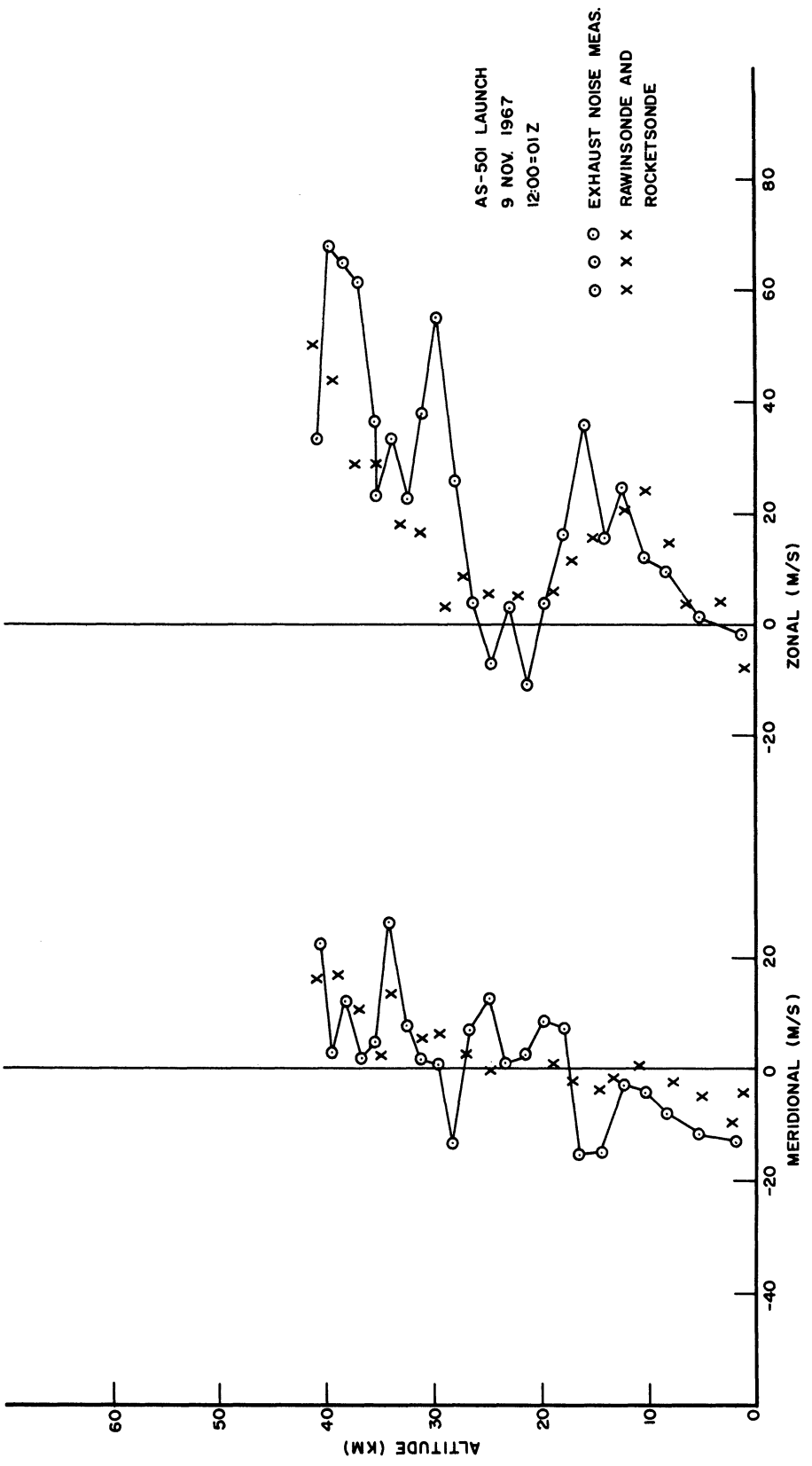

Figure 19. Wind profile, AS-501, 9 November 1967.

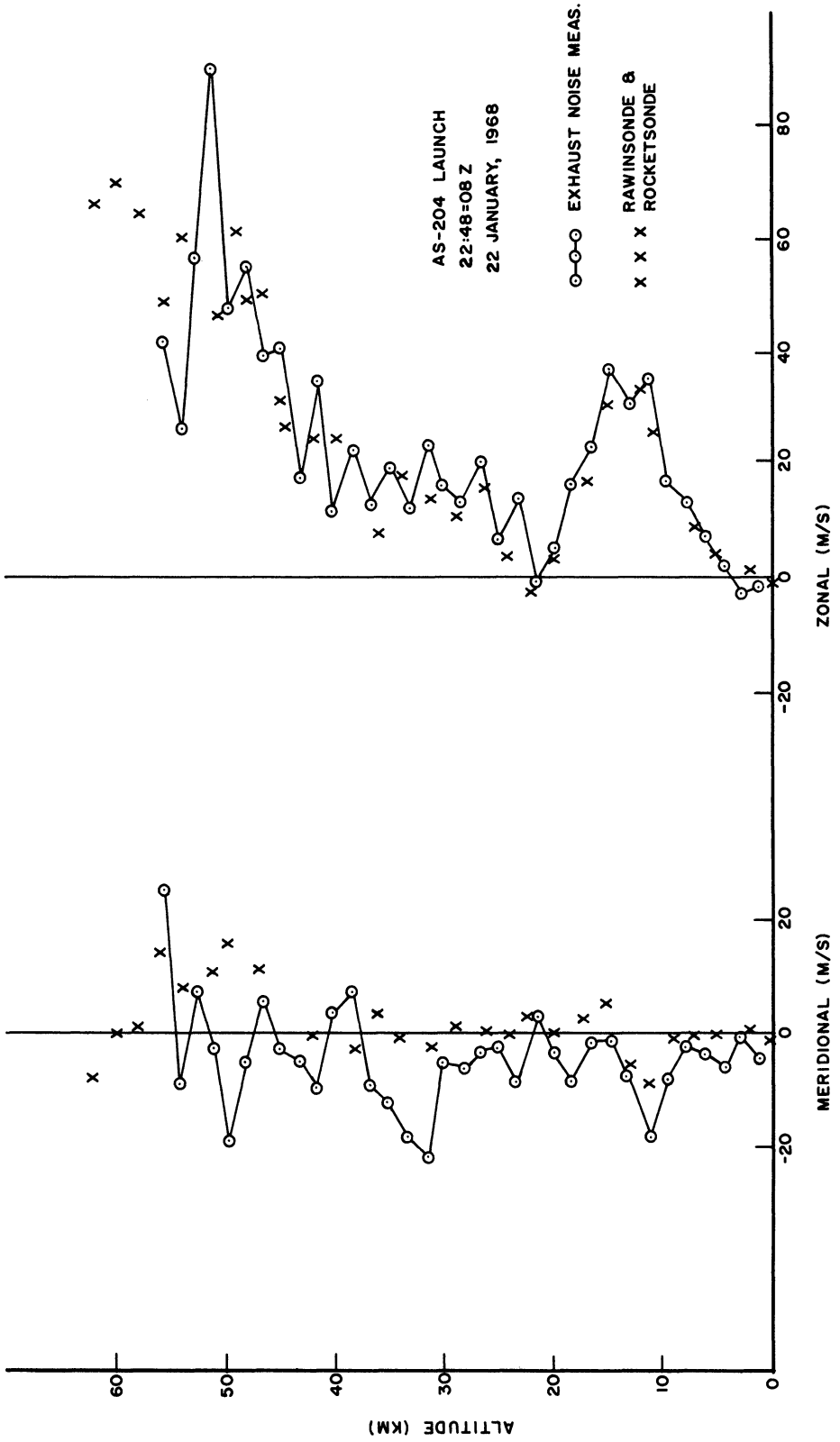

Figure 20. Wind profile, AS-204, 22 January 1968.

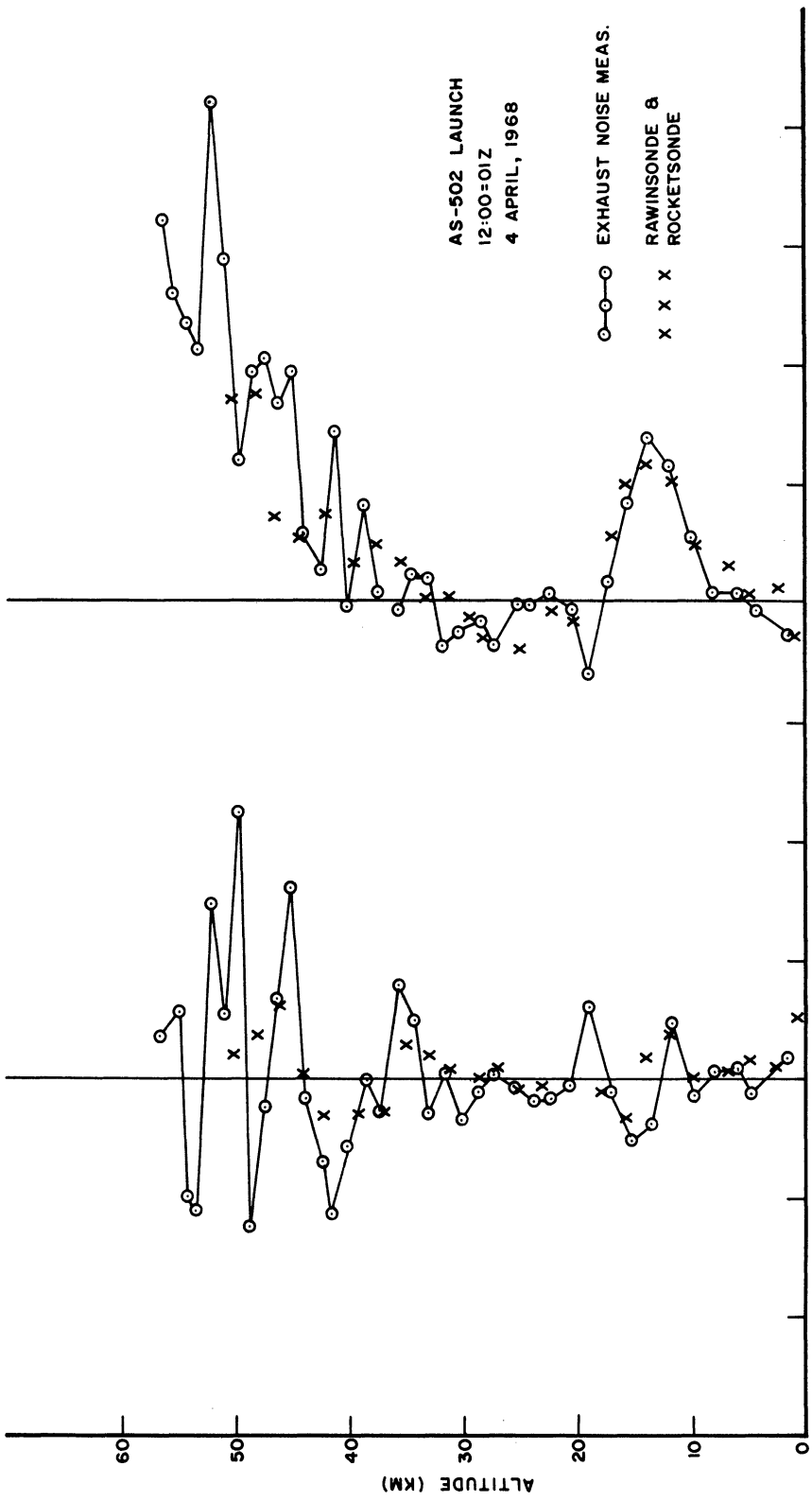

Figure 21. Wind profile, AS-502, 4 April 1968.

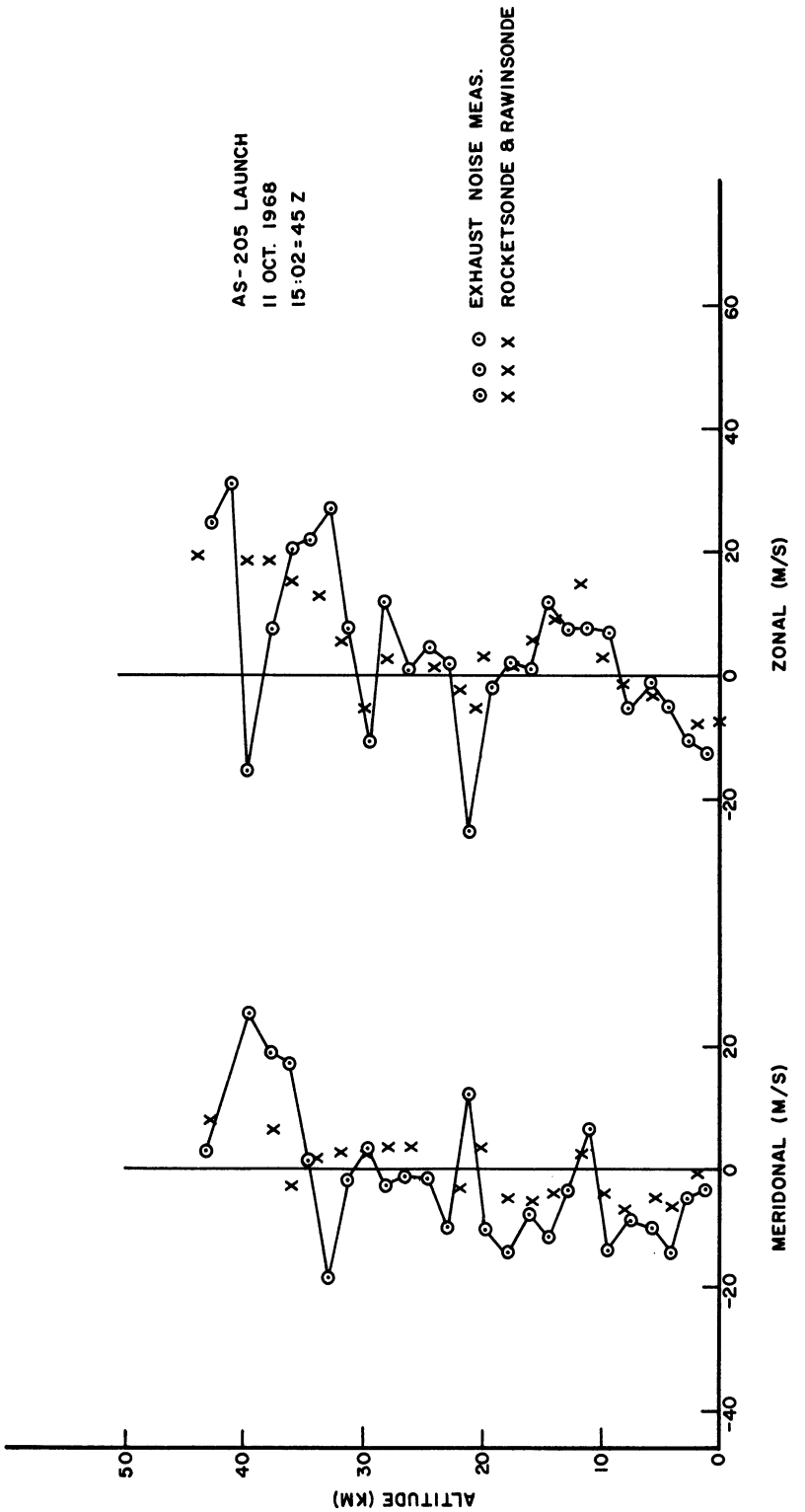

Figure 22. Wind profile, AS-205, 11 October 1968.

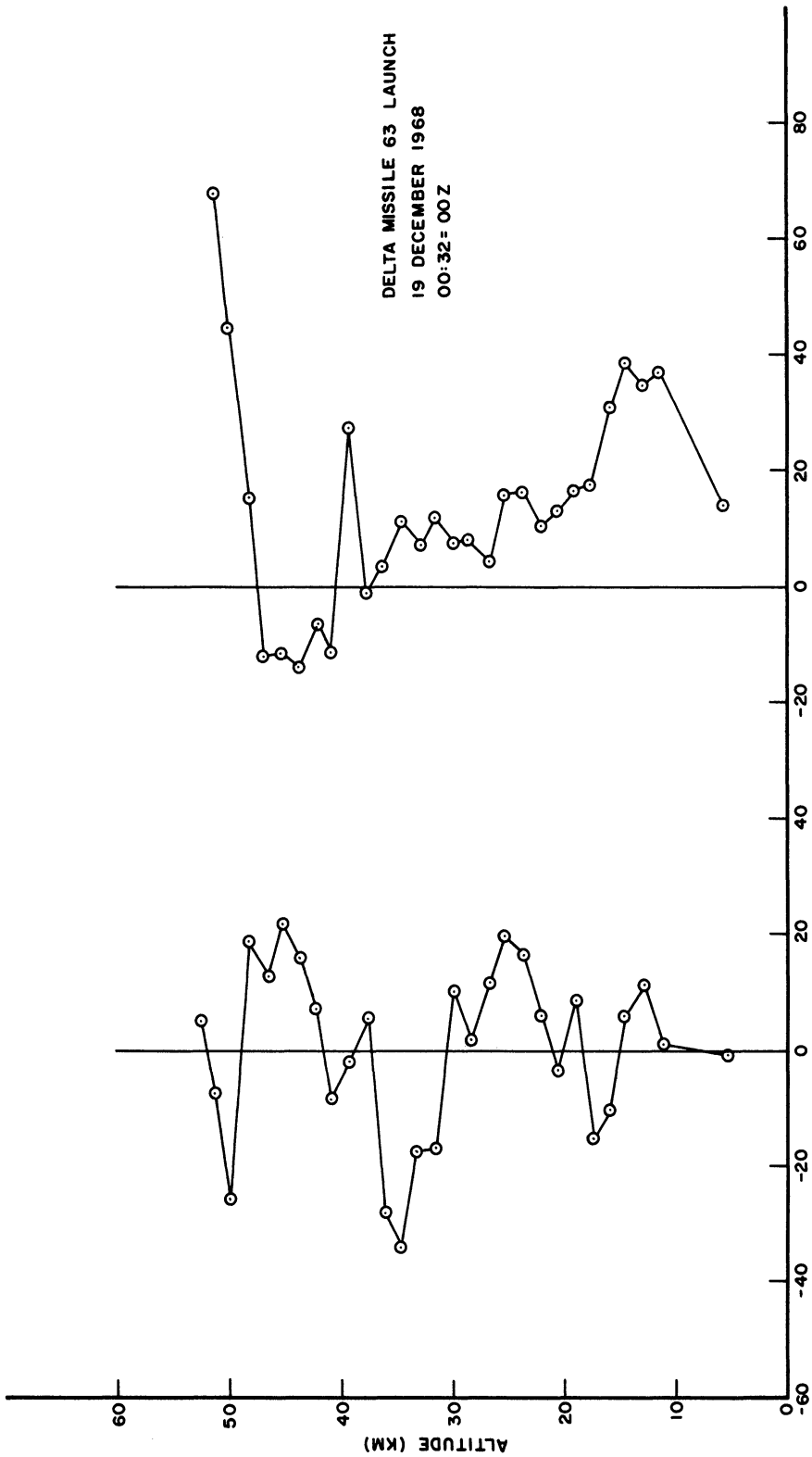

Figure 23. Wind profile, Delta 63, 19 December 1968.

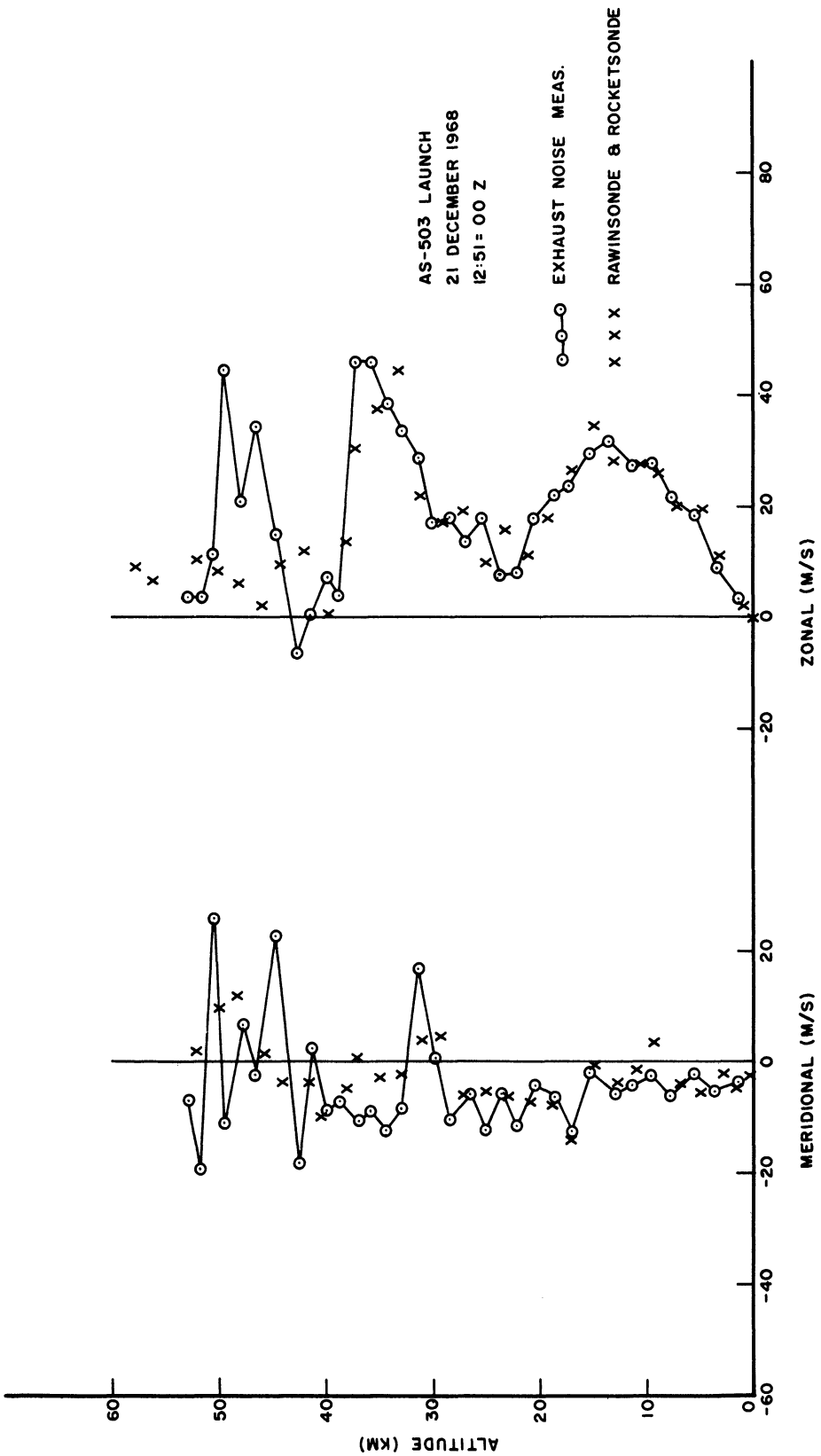

Figure 24. Wind profile, AS-503, 21 December 1968.

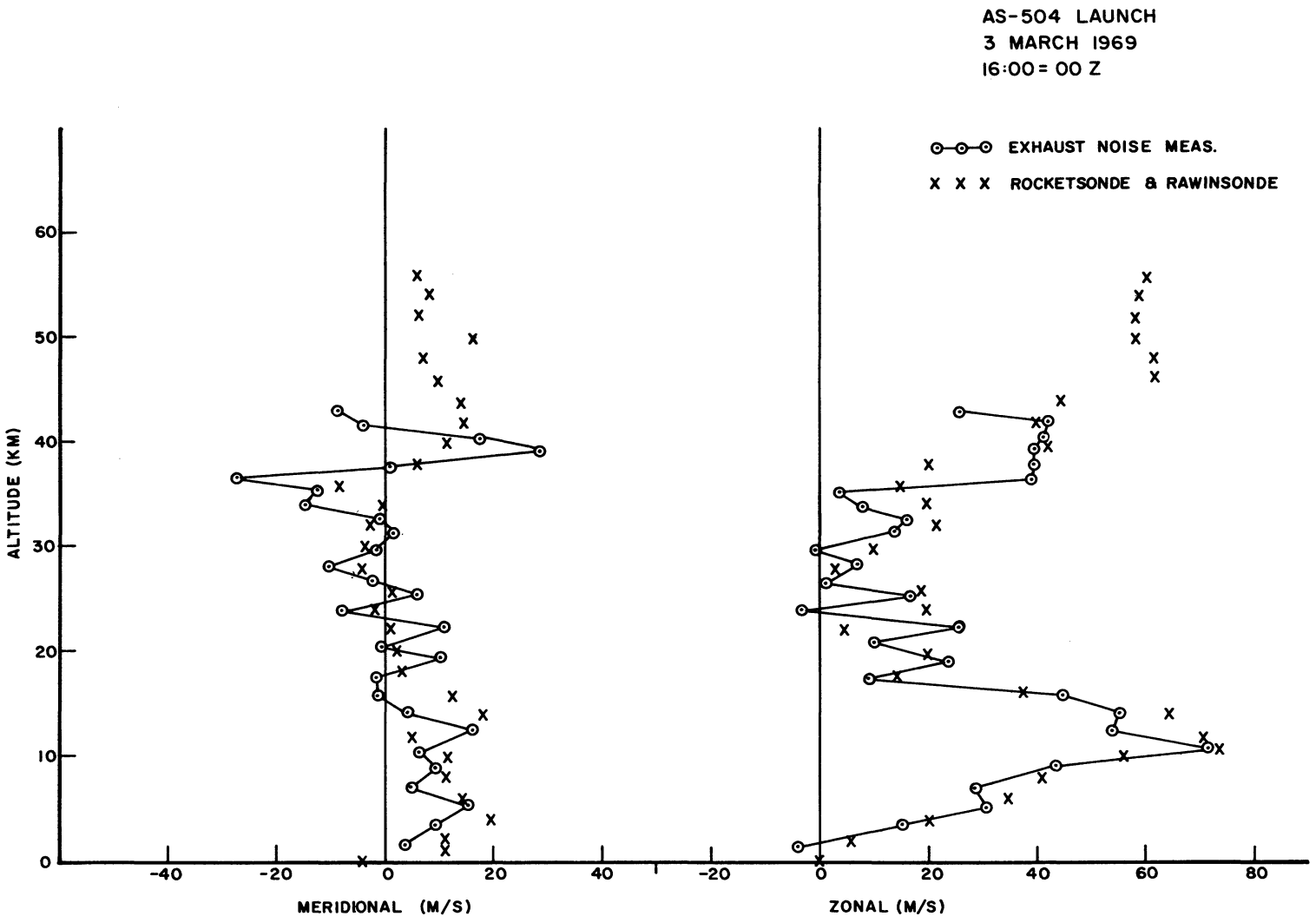

Figure 25. Wind profile, AS-504, 3 March 1969.

4. FAR-FIELD ACOUSTIC WIND MEASUREMENT

G. V. Groves has developed a generalized method of geometric ray acoustics and has shown that the characteristic velocities appear in the ray equation as constants of integration. Thus, they do not need to be converted into the direction of arrival of the wavefront and neither is there a requirement for an independently determined temperature or speed of sound profile. This analysis permits wider microphone spacing with the advantages that the difference between sound ray travel times is increased and the effective timing accuracy is improved. Furthermore, the microphones can be placed randomly rather than positioned along two axes. In order to obtain accurate results at higher altitudes the microphones must be farther apart than they are in the present array. This distance should be increased to about 8-12 km. This method allows for complete generalization of microphone positions provided the deviations from a horizontal plane are quite small compared to the height of the noise source. Variations in height of the microphones are taken into account in the first order analysis. Second and higher order effects arising from supersonic velocity and refraction effects are also taken into account.

In Figure 26, x, y, and z are the coordinates of a noise event that occurred at time T sec after launch; x_i, y_i, and z_i are the coordinates of the i^{th} microphone and τ_i is the total elapsed time from lift-off to the sound arrival at the i^{th} microphone; v is the speed of sound; and w_x, w_y, and w_z are wind components considered constant in a layer.

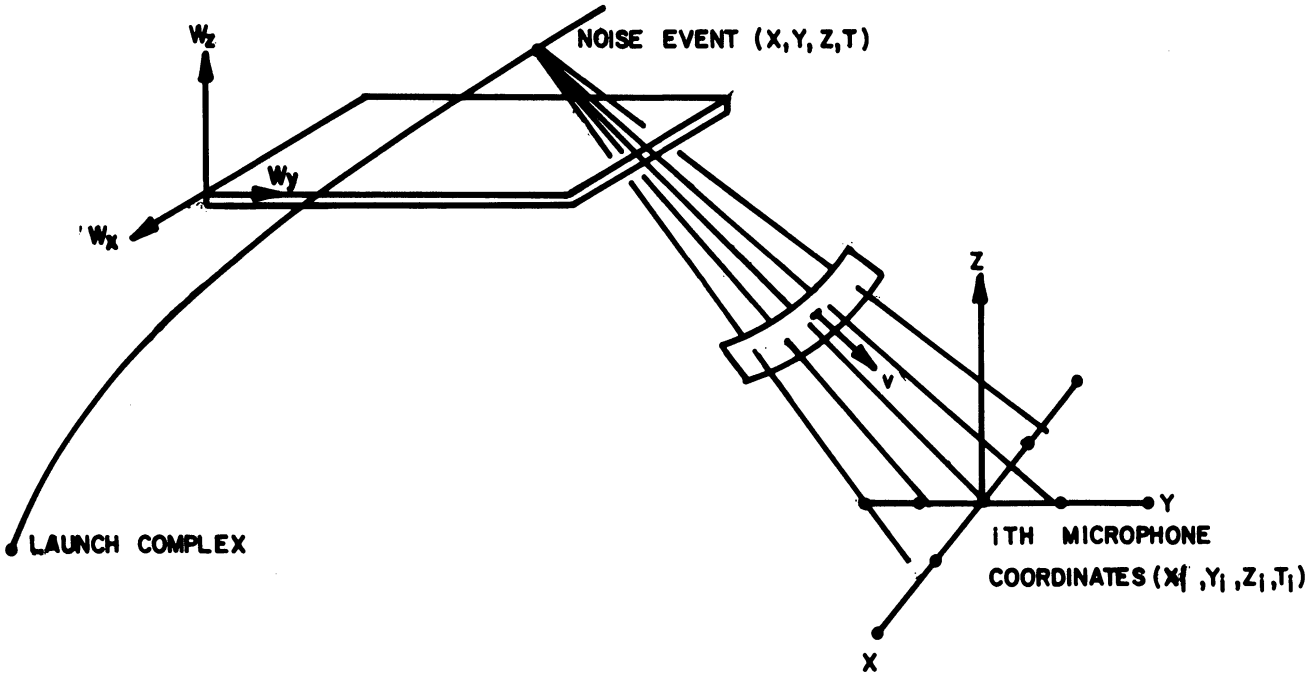

Figure 26. Incoming acoustic wavefront.

Groves has derived expressions for a case of propagation velocity of disturbance, vM(T), where M(T) is the Mach number of shock wave rapidly tending to unity and also taking into account the refraction effects. Integrated values of three wind components and speed of sound are defined:

$$W_x = \int_o^z w_x dz \; ; \quad W_y = \int_o^z w_y dz \; ; \quad W_z = \int_o^z w_y dz \; ; \quad V = \int_o^z v dz \; . \qquad (4.1)$$

Groves has shown that

$$V^2(1+\epsilon) = \left(W_x + \frac{X_i Z_i}{\tau_i - T}\right)^2 + \left(W_y + \frac{Y_i Z_i}{\tau_i - T}\right)^2 + \left(W_z + \frac{Z_i^2}{\tau_i - T}\right)^2 \qquad (4.2)$$

where $X_i = x - x_i$,

$Y_i = y - y_i$,

$Z_i = z - z_i$,

ϵ = second and higher order effects.

If equation (4.2) is considered only to the first order, ϵ may be ignored. The error, by making $\epsilon = 0$, is less than one percent. Expanding (4.2) gives

$$V^2 - W_x^2 - W_y^2 - W_z^2 = 2W_x \frac{X_i Z_i}{\tau_i - T} + \left(\frac{X_i Z_i}{\tau_i - T}\right)^2 + 2W_y \frac{Y_i Z_i}{\tau_i - T} + \left(\frac{Y_i Z_i}{\tau_i - T}\right)^2 + 2W_z \frac{Z_i^2}{\tau_i - T} + \frac{Z_i^4}{(\tau_i - T)^2} . \quad (4.3)$$

If all microphones are essentially in a horizontal plane, $z_i \cong 0$; and since wind components and speed of sound are assumed constant in a layer,

$$W_x = w_x z \; ; \quad W_y = w_y z \; ; \quad W_z = w_z z \; ; \quad V = vz . \quad (4.4)$$

Equation (4.3) becomes

$$v^2 - w_x^2 - w_y^2 - w_z^2 = 2w_x \frac{x-x_i}{\tau_i - T} + 2w_y \frac{y-y_i}{\tau_i - T} + 2w_z \frac{z-z_i}{\tau_i - T} + \left(\frac{x-x_i}{\tau_i - T}\right)^2 + \left(\frac{y-y_i}{\tau_i - T}\right)^2 + \left(\frac{z-z_i}{\tau_i - T}\right)^2 . \quad (4.5)$$

Let $v^2 - w_x^2 - w_y^2 - w_z^2 = Q$ for simplicity and

$$\frac{x-x_i}{\tau_i - T} = a_i \; ,$$

$$\frac{y-y_i}{\tau_i - T} = b_i \; ,$$

$$\frac{z-z_i}{\tau_i - T} = c_i \; ;$$

$$w_x = u ,$$

$$w_y = v ,$$

$$w_z = w .$$

Equation (4.5) becomes

$$Q - 2a_i u - 2b_i v - 2c_i w = a_i^2 + b_i^2 + c_i^2 . \tag{4.6}$$

For a number of microphones, N, equation (4.6) is to be solved for unknowns Q, u, v, and w such that

$$F = \left\{ NQ - 2u \sum_{i=1}^{N} a_i - 2v \sum_{i=1}^{N} b_i - 2w \sum_{i=1}^{N} c_i - \left[\sum_{i=1}^{N} a_i + \sum_{i=1}^{N} b_i + \sum_{i=1}^{N} c_i \right] \right\}^2 \tag{4.7}$$

is a minimum. Let

$$f_i = Q - 2a_i u - 2b_i v - 2c_i w - a_i^2 - b_i^2 - c_i^2 ,$$

so

$$F = \left[\Sigma f_i \right]^2 ,$$

then

$$\frac{\partial F}{\partial Q} = 0 \tag{4.8}$$

gives

$$\Sigma f_i = 0 ;$$

$$\frac{\partial F}{\partial u} = 0$$

gives

$$\Sigma a_i f_i = 0 ; \tag{4.9}$$

$$\frac{\partial F}{\partial V} = 0$$

gives

$$\Sigma b_i f_i = 0 \; ; \tag{4.10}$$

and

$$\frac{\partial F}{\partial w} = 0$$

gives

$$\Sigma c_i f_i = 0 \; . \tag{4.11}$$

Equations (4.8), (4.9), (4.10) and (4.11) can be written as

$$NQ - 2u\Sigma a_i - 2v\Sigma b_i - 2w\Sigma c_i = \Sigma a_i^2 + \Sigma b_i^2 + \Sigma c_i^2 \; , \tag{4.12}$$

$$Q\Sigma a_i - 2u\Sigma a_i^2 - 2v\Sigma a_i b_i - 2w\Sigma a_i c_i = \Sigma a_i^3 + \Sigma a_i b_i^2 + \Sigma a_i c_i^2 \; , \tag{4.13}$$

$$Q\Sigma b_i - 2u\Sigma a_i b_i - 2v\Sigma b_i^2 - 2w\Sigma b_i c_i = \Sigma a_i^2 b_i + \Sigma b_i^3 + \Sigma b_i c_i^2 \; , \tag{4.14}$$

$$Q\Sigma c_i - 2u\Sigma a_i c_i - 2v\Sigma b_i c_i - 2w\Sigma c_i^2 = \Sigma a_i^2 c_i + \Sigma c_i b_i^2 + \Sigma c_i^3 \; . \tag{4.15}$$

Equations (4.12), (4.13), (4.14), and (4.15) are linear simultaneous equations with unknowns Q, u, v and w.

Initially, we choose a value of T, which gives x, y, and z from the trajectory. Thus, knowing a_i, b_i, and c_i, we can solve for Q, u, v, and w. Then we choose another T and determine Q, u, v, and w again. We repeat the solution with a small increment in T until we find Q, u, and v with $w \tilde{=} 0$. This will be the correct solution within our assumptions,

$$v = \sqrt{Q+u^2+v^2+w^2} .$$

In this way the average speed of sound (and thus the average temperature) and two wind components are determined in a layer.

5. SUMMARY

The acoustic wind measurement system is now fully operational and capable of acquiring data on all large rocket launches at Cape Kennedy. The wind profiles determined by this system are in agreement with other simultaneous measurements, thereby establishing the validity of the technique. On the basis of an extensive error analysis (Bushman, Kakli, and Graves, 1968), the maximum error was found to average about 10 m/sec in each component. These errors are attributed principally to inaccuracies in determining sound arrival times. These errors could probably be reduced by more sophisticated measurement and data reduction techniques. At this time it is not felt that the increased computer time and costs can be justified by the error reduction that would be achieved.

The measurement system as it stands now could be significantly improved by the addition of far-field sites discussed in Section 4. This addition would eliminate the requirement for separate determination of speed of sound profiles. New acoustic microphones have been developed with more sensitivity and with a flat response over a wider frequency range. Implementation of these microphones would also improve the system. These microphones have all the required electronics self-contained and would eliminate the need for any additional equipment with the exception of recorders. By using the new acoustic microphones, the system would essentially be entirely portable. The output of one of these new microphones was recorded during the launch of AS-505 (Apollo 10) to determine whether it would be compatible with the present system. The results were

not available in time to include in this report but will be included in a supplementary report containing the results of AS-505 (Apollo 10) and AS-506 (Apollo 11).

Since its inception in 1965, the acoustic wind measuring technique has been developed and tested and the system has been improved to the point of being a fully operational and essentially automatic system.

6. BIBLIOGRAPHY

Bushman, W. W., The Acoustic Wind Measurement: A Six Month Summary, Space Physics Research Laboratory, Technical Report 07871-1-T, Contract NAS 8-20357, September 1966.

Bushman, W. W., Carignan, G. R., Kakli, G. M., and Smith. O. E., "High Altitude Wind Measurements from Rocket Exhaust Noise," Journal of Geophysical Research, Vol. 73, No. 15, August 1, 1968, pp. 4969-4977.

Bushman, W. W., Kakli, G. M., and Carignan, G. R., An Acoustic Wind Measuring Technique, Space Physics Research Laboratory, Technical Report 05911-2-T, Contract NAS8-11054, July 1965.

Bushman, W. W., Kakli, G. M., and Graves, M. E., The Acoustic Wind Measurement, Space Physics Research Laboratory, Technical Report 07871-2-T, Contract NAS8-20357, February 1968.

Bushman, W. W., and Smith, O. E., An Acoustic Wind Measuring Technique, Fourth Aerospace Sciences Meeting, Los Angeles, California, July 27-29, 1966, AIAA Paper No. 66-440.

Dyer, Ira, "Distribution of Sound Sources in a Jet Stream," Journal of the Acoustical Society of America, 31, p. 1016, 1959.

Groves, G. V., "Introductory Theory for Upper Atmosphere Wind and Sonic Velocity Determination by Sound Propagation," Journal of Atmospheric and Terrestrial Physics, 8, pp. 24-38, 1956.

Groves, G. V., "Theory of the Rocket Grenade Method of Determining Upper Atmosphere Properties by Sound Propagation," Journal of Atmospheric and Terrestrial Physics, 8, pp. 189-203, 1956.

Milne, E. A., "Sound Waves in the Atmosphere," Philosophical Magazine, 42, p. 96, 1921.

Nordberg, W., and Smith, W., The Rocket-Grenade Experiment, NASA Technical Note D-2107, March 1964.

Otterman, J., A Simplified Method of Computing Upper Atmosphere Temperature and Winds in the Rocket-Grenade Experiment, The University of Michigan, Technical Report 2387-40-T, Army contract No. DA-36-039-SC-64657, June 1958.

Smith, O. E., and Weidner, D K., A Reference Atmosphere for Patrick AFB, Florida (annual revision, 1963), NASA TM X-53139, September 1964.

Stroud, W. G., Nordberg, W., and Walsh, J. R., "Atmospheric Temperatures and Winds between 30 and 80 Km," Journal of Geophysical Research, 61, p. 45, 1956.